# Statistical Early Warning Models with Applications: Supplementary Material

Lucas P. Harlaar[*],
*Statistics Netherlands, Maastricht University, Vrije Universiteit Amsterdam*
Jacques J.F. Commandeur,
*SWOV Institute for Road Safety Research, Vrije Universiteit Amsterdam*
Jan A. van den Brakel,
*Statistics Netherlands, Maastricht University*
Siem Jan Koopman,
*Vrije Universiteit Amsterdam, Tinbergen Institute*
Niels Bos,
*SWOV Institute for Road Safety Research*
Frits D. Bijleveld,
*SWOV Institute for Road Safety Research, Vrije Universiteit Amsterdam*

August 27, 2025

# SA Supplementary material Section 2

## SA.1 Statistical Early Warning Model

We start off from the state space approach for the analysis of time series data, see Harvey (1989), Durbin and Koopman (2012), and Commandeur and Koopman (2007). An important motivation for opting for this methodology is that it easily handles missing data in time series, and transparently generalizes to the analysis of multivariate time series. Let $\boldsymbol{y}_t$ denote the $N \times 1$ observation vector that contains the $N$ observations at time $t$. The general linear Gaussian state space model for the $T$-dimensional observation sequence $\boldsymbol{y}_1, \ldots, \boldsymbol{y}_T$ is given by

$$\boldsymbol{y}_t = \boldsymbol{Z}_t \boldsymbol{\alpha}_t + \boldsymbol{\varepsilon}_t, \qquad \boldsymbol{\varepsilon}_t \sim \text{NID}(\boldsymbol{0}, \boldsymbol{H}_t), \tag{SA.1}$$

$$\boldsymbol{\alpha}_{t+1} = \boldsymbol{T}_t \boldsymbol{\alpha}_t + \boldsymbol{R}_t \boldsymbol{\eta}_t, \qquad \boldsymbol{\eta}_t \sim \text{NID}(\boldsymbol{0}, \boldsymbol{Q}_t), \qquad t = 1, \ldots, T, \tag{SA.2}$$

where $\boldsymbol{\alpha}_t$ is the state vector, $\boldsymbol{\varepsilon}_t$ and $\boldsymbol{\eta}_t$ are disturbance vectors and the system matrices $\boldsymbol{Z}_t$, $\boldsymbol{T}_t$, $\boldsymbol{R}_t$, $\boldsymbol{H}_t$ and $\boldsymbol{Q}_t$ are fixed and known but a selection of elements may depend on

[*]Corresponding author: Department of Quantitative Economics, Maastricht University, P.O. Box 616, 6200 MD Maastricht, The Netherlands. E-mail: lucas.harlaar@maastrichtuniversity.nl

an unknown parameter vector. Equation (SA.1) is called the *observation* or *measurement equation*, while (SA.2) is called the *state* or *transition equation*. The $M \times 1$ state vector $\boldsymbol{\alpha}_t$ is unobserved. The $N \times 1$ irregular vector $\boldsymbol{\varepsilon}_t$ has zero mean and $N \times N$ variance matrix $\boldsymbol{H}_t$.

The $N \times M$ matrix $\boldsymbol{Z}_t$ links the observation vector $\boldsymbol{y}_t$ with the unobservable state vector $\boldsymbol{\alpha}_t$. Besides the state variables that define the trend, seasonal and cycle, $\boldsymbol{\alpha}_t$ may also consist of regression variables. The $M \times M$ transition matrix $\boldsymbol{T}_t$ in (SA.2) determines the dynamic evolution of the state vector. The $R \times 1$ disturbance vector $\boldsymbol{\eta}_t$ for the state vector update has zero mean and $R \times R$ variance matrix $\boldsymbol{Q}_t$. The observation and state disturbances $\boldsymbol{\varepsilon}_t$ and $\boldsymbol{\eta}_t$ are assumed to be serially independent and independent of each other at all time points. In many standard cases, $R = M$ and matrix $\boldsymbol{R}_t$ is the identity matrix $I_M$. In other cases, matrix $\boldsymbol{R}_t$ is an $M \times R$ selection matrix with $R < M$. Although matrix $\boldsymbol{R}_t$ can be specified freely, it is often composed of a selection from the first $R$ columns of the identity matrix $I_M$.

By appropriate choices of the vectors $\boldsymbol{\alpha}_t$, $\boldsymbol{\varepsilon}_t$ and $\boldsymbol{\eta}_t$, and of the matrices $\boldsymbol{Z}_t$, $\boldsymbol{T}_t$, $\boldsymbol{H}_t$, $\boldsymbol{R}_t$ and $\boldsymbol{Q}_t$, a wide range of different time series models can be derived from (SA.1) and (SA.2). In this paper we discuss the class of *seemingly unrelated time series equations* (SUTSE) models, which can be considered a multivariate extension of structural time series models:

$$\boldsymbol{y}_t = \boldsymbol{\mu}_t + \boldsymbol{\gamma}_t + \boldsymbol{\varepsilon}_t, \qquad \boldsymbol{\varepsilon}_t \sim \text{NID}(\boldsymbol{0}, \boldsymbol{\Sigma}_\varepsilon), \tag{SA.3}$$

where $\boldsymbol{y}_t$ is a $N \times 1$ vector of time series, $\boldsymbol{\mu}_t$ is a $N \times 1$ vector of unobserved trends, $\boldsymbol{\gamma}_t$ is a $N \times 1$ vector of unobserved seasonal effects and $\boldsymbol{\varepsilon}_t$ is a $N \times 1$ vector of the irregular or noise component. The trend is defined as the *local linear trend* model, where the trend consists of a stochastic level and slope component,

$$\boldsymbol{\mu}_{t+1} = \boldsymbol{\mu}_t + \boldsymbol{\nu}_t + \boldsymbol{\xi}_t, \qquad \boldsymbol{\xi}_t \sim \text{NID}(\boldsymbol{0}, \boldsymbol{\Sigma}_\xi), \tag{SA.4}$$

$$\boldsymbol{\nu}_{t+1} = \boldsymbol{\nu}_t + \boldsymbol{\zeta}_t, \qquad \boldsymbol{\zeta}_t \sim \text{NID}(\boldsymbol{0}, \boldsymbol{\Sigma}_\zeta). \tag{SA.5}$$

More parsimonious trend models can be obtained straightforwardly by restricting the $N \times N$ covariance matrices $\boldsymbol{\Sigma}_\xi$ or $\boldsymbol{\Sigma}_\zeta$ to be equal to $\boldsymbol{0}$. The seasonal process can be modelled as a *dummy seasonal* model,

$$\boldsymbol{\gamma}_{t+1} = -\sum_{j=1}^{s-1} \boldsymbol{\gamma}_{t+1-j} + \boldsymbol{\omega}_t, \qquad \boldsymbol{\omega}_t \sim \text{NID}(\boldsymbol{0}, \boldsymbol{\Sigma}_\omega), \tag{SA.6}$$

where $s$ equals the number of months or quarters per year, depending on the frequency of the time series. Alternatively, a *trigonometric seasonal* model can be used,

$$\boldsymbol{\gamma}_t = \sum_{j=1}^{(s/2)} \boldsymbol{\gamma}_{j,t}, \tag{SA.7}$$

where

$$\begin{aligned} \boldsymbol{\gamma}_{j,t+1} &= \cos\left(\frac{2\pi j}{s}\right) \boldsymbol{\gamma}_{j,t} + \sin\left(\frac{2\pi j}{s}\right) \boldsymbol{\gamma}^*_{j,t} + \boldsymbol{\omega}_{j,t}, \\ \boldsymbol{\gamma}^*_{j,t+1} &= -\sin\left(\frac{2\pi j}{s}\right) \boldsymbol{\gamma}_{j,t} + \cos\left(\frac{2\pi j}{s}\right) \boldsymbol{\gamma}^*_{j,t} + \boldsymbol{\omega}^*_{j,t}, \qquad j = 1, \ldots, (s/2), \end{aligned} \tag{SA.8}$$

and where the trigonometric functions are scalars, $\boldsymbol{\gamma}_{j,t}$ and $\boldsymbol{\gamma}^*_{j,t}$ are $N \times 1$ vectors and $\boldsymbol{\omega}_{j,t}$ and $\boldsymbol{\omega}^*_{j,t}$ are independent NID$(\mathbf{0}, \boldsymbol{\Sigma}_\omega)$ variables. The disturbance terms of the different components in (SA.3), (SA.4), (SA.5) and (SA.6) or (SA.8) are mutually independent. However, the model allows for cross-sectional correlations in the disturbances within these components. In other words, $\boldsymbol{\Sigma}_\xi$, $\boldsymbol{\Sigma}_\zeta$ and $\boldsymbol{\Sigma}_\omega$ can be diagonal, full rank or rank deficient (i.e., a matrix with rank less than full).

In case of rank deficient covariance matrices, the SUTSE model from (SA.3) can be written as a common factor model, in which some or all of the components are driven by disturbance vectors with less than $N$ elements:

$$\boldsymbol{y}_t = \boldsymbol{\Theta}_\mu \boldsymbol{\mu}^\dagger_t + \boldsymbol{\Theta}_\nu \boldsymbol{\mu}^{\dagger\dagger}_t + \boldsymbol{\mu}_{\theta,t} + \boldsymbol{\Theta}_\gamma \boldsymbol{\gamma}^\dagger_t + \boldsymbol{\gamma}_{\theta,t} + \boldsymbol{\varepsilon}_t, \qquad \boldsymbol{\varepsilon}_t \sim \text{NID}(\mathbf{0}, \boldsymbol{\Sigma}_\varepsilon), \tag{SA.9}$$

$$\boldsymbol{\mu}^\dagger_{t+1} = \boldsymbol{\mu}^\dagger_t + \boldsymbol{\xi}^\dagger_t, \qquad \boldsymbol{\xi}^\dagger_t \sim \text{NID}(\mathbf{0}, \boldsymbol{\Sigma}^\dagger_\xi), \tag{SA.10}$$

$$\boldsymbol{\mu}^{\dagger\dagger}_{t+1} = \boldsymbol{\mu}^{\dagger\dagger}_t + \boldsymbol{\nu}^{\dagger\dagger}_t, \tag{SA.11}$$

$$\boldsymbol{\nu}^{\dagger\dagger}_{t+1} = \boldsymbol{\nu}^{\dagger\dagger}_t + \boldsymbol{\zeta}^{\dagger\dagger}_t, \qquad \boldsymbol{\zeta}^{\dagger\dagger}_t \sim \text{NID}(\mathbf{0}, \boldsymbol{\Sigma}^{\dagger\dagger}_\zeta), \tag{SA.12}$$

where $\boldsymbol{\mu}^\dagger_t$ is a $K_\mu \times 1$ vector of common levels, modelled as in (SA.4) with $\boldsymbol{\nu}^\dagger_t$ equal to $\mathbf{0}$ for all $t$ and diagonal $\boldsymbol{\Sigma}^\dagger_\xi$, $\boldsymbol{\mu}^{\dagger\dagger}_t$ is a $K_\nu \times 1$ vector of common slopes, modelled as in (SA.4) and (SA.5) without a vector with level disturbance terms and diagonal $\boldsymbol{\Sigma}^{\dagger\dagger}_\zeta$ and $\boldsymbol{\gamma}^\dagger_t$ is a $K_\gamma \times 1$ vector of common seasonals, modelled as in (SA.6) or (SA.7) and (SA.8) and diagonal $\boldsymbol{\Sigma}^\dagger_\omega$. The $N \times 1$ vector $\boldsymbol{\mu}_{\theta,t}$ consists of $\min(K_\mu, K_\nu)$ zeros as first elements followed by a $\max(K_\mu, K_\nu) - \min(K_\mu, K_\nu)$ vector $\bar{\boldsymbol{\mu}}$ or $\bar{\boldsymbol{\nu}}t$, depending on the rank discrepancy between the level and slope, and a $N - \min(K_\mu, K_\nu)$ vector $\bar{\boldsymbol{\mu}} + \bar{\boldsymbol{\nu}}t$ of fixed linear trends as remainder. The $N \times 1$ vector $\gamma_{\boldsymbol{\theta},t}$ consists of $K_\gamma$ zeros as first elements followed by a $N - K_\gamma$ vector of fixed seasonal effects as remainder, i.e. $\bar{\boldsymbol{\gamma}}_t = \bar{\boldsymbol{\gamma}}_j$ if $t$ corresponds to seasonal period $j$, for $j = 1, \ldots, s$. The $N \times K_\mu$ factor loading matrix $\boldsymbol{\Theta}_\mu$ has the $ij$-th element $\theta_{ij}$ equal to zero for $j > i$ and $\theta_{ii}$ equal to one. Similar structures apply to $\boldsymbol{\Theta}_\nu$ and $\boldsymbol{\Theta}_\gamma$. Note that we can obtain the original SUTSE notation (SA.3) by writing $\boldsymbol{\mu}_t = \boldsymbol{\Theta}_\mu \boldsymbol{\mu}^\dagger_t + \boldsymbol{\Theta}_\nu \boldsymbol{\mu}^{\dagger\dagger}_t + \boldsymbol{\mu}_{\theta,t}$ and $\boldsymbol{\gamma}_t = \boldsymbol{\Theta}_\gamma \boldsymbol{\gamma}^\dagger_t + \boldsymbol{\gamma}_{\theta,t}$, while $\boldsymbol{\Sigma}_\xi = \boldsymbol{\Theta}_\mu \boldsymbol{\Sigma}^\dagger_\xi \boldsymbol{\Theta}'_\mu$, $\boldsymbol{\Sigma}_\zeta = \boldsymbol{\Theta}_\nu \boldsymbol{\Sigma}^{\dagger\dagger}_\zeta \boldsymbol{\Theta}'_\nu$ and $\boldsymbol{\Sigma}_\gamma = \boldsymbol{\Theta}_\gamma \boldsymbol{\Sigma}^\dagger_\omega \boldsymbol{\Theta}'_\gamma$ are singular matrices with rank $K_\mu$, $K_\nu$ and $K_\gamma$ respectively (Harvey and Koopman 1997; Koopman, Harvey, Doornik, and Shephard 2009).

## SA.2 Labour Force model state space form

The Labour Force model can also be written in linear state space form from (SA.1)-(SA.2). The measurement equation can be written as:

$$\begin{pmatrix} y_t \\ x_{t,1} \\ x_{t,2} \\ x_{t,3} \end{pmatrix} = \begin{bmatrix} \begin{pmatrix} 1 & 0 & 1 & 0 & 0 \end{pmatrix} \otimes \boldsymbol{I}_4 & \begin{pmatrix} 0 & 0 & 0 \\ k_{t,1} & 0 & 0 \\ 0 & k_{t,2} & 0 \\ 0 & 0 & k_{t,3} \end{pmatrix} \end{bmatrix} \boldsymbol{\alpha}_t + \begin{pmatrix} \varepsilon_{t,y} \\ \varepsilon_{t,1} \\ \varepsilon_{t,2} \\ \varepsilon_{t,3} \end{pmatrix}, \tag{SA.13}$$

where the state vector $\boldsymbol{\alpha}_t$ is specified as follows:

$$\boldsymbol{\alpha}_t = \begin{pmatrix} \boldsymbol{\mu}'_t & \boldsymbol{\nu}'_t & \boldsymbol{\gamma}'_t & \boldsymbol{u}'_t \end{pmatrix}', \quad \boldsymbol{\mu}_t = \begin{pmatrix} \mu_{t,y} & \mu_{t,x_1} & \mu_{t,x_2} & \mu_{t,x_3} \end{pmatrix}', \quad \boldsymbol{\nu}_t = \begin{pmatrix} \nu_{t,y} & \nu_{t,x_1} & \nu_{t,x_2} & \nu_{t,x_3} \end{pmatrix}',$$
$$\boldsymbol{\gamma}_t = \begin{pmatrix} \gamma_{t,y} & \gamma_{t,x_1} & \gamma_{t,x_2} & \gamma_{t,x_3} & \cdots & \gamma_{t-2,y} & \gamma_{t-2,x_1} & \gamma_{t-2,x_2} & \gamma_{t-2,x_3} \end{pmatrix}', \quad \boldsymbol{u}_t = \begin{pmatrix} u_{t,1} & u_{t,2} & u_{t,3} \end{pmatrix}',$$

which contains the trend, dummy seasonal and sampling error terms. As discussed the idiosyncratic noise of the target and LFS auxiliary series are Gaussian i.i.d. sequences with the following diagonal irregular covariance matrix:

$$\boldsymbol{\Sigma}_{\varepsilon} = \begin{bmatrix} \sigma^2_{\varepsilon_y} & 0 & 0 & 0 \\ 0 & \sigma^2_{\varepsilon_x} & 0 & 0 \\ 0 & 0 & \sigma^2_{\varepsilon_x} & 0 \\ 0 & 0 & 0 & \sigma^2_{\varepsilon_x} \end{bmatrix}. \tag{SA.14}$$

The state vector's dynamic transitioning can be described as follows:

$$\boldsymbol{\alpha}_{t+1} = \begin{bmatrix} \begin{pmatrix} \boldsymbol{T}_{\mu} & \mathbf{0}_{8\times 12} \\ \mathbf{0}_{12\times 8} & \boldsymbol{T}_{\gamma} \end{pmatrix} & \mathbf{0}_{20\times 3} \\ \mathbf{0}_{3\times 20} & \begin{pmatrix} \phi & 0 & 0 \\ 0 & \phi & 0 \\ 0 & 0 & \phi \end{pmatrix} \end{bmatrix} \boldsymbol{\alpha}_t + \boldsymbol{\eta}_t, \qquad \boldsymbol{\eta}_t \sim \mathbf{N}(\mathbf{0}, \boldsymbol{\Sigma}_{\eta}), \tag{SA.15}$$

where $\phi$ is the monthly autoregressive coefficient of the sampling error, retrieved from van den Brakel and Michiels (2021) and treated as known. We opt for a local linear trend model and a stochastic seasonal dummy model, see Harvey (1989) and Durbin and Koopman (2012), by specifying:

$$\boldsymbol{T}_{\mu} = \begin{bmatrix} 1 & 1 \\ 0 & 1 \end{bmatrix} \otimes \boldsymbol{I}_4, \quad \boldsymbol{T}_{\gamma} = \begin{bmatrix} -1 & -1 & -1 \\ 1 & 0 & 0 \\ 0 & 1 & 0 \end{bmatrix} \otimes \boldsymbol{I}_4, \quad \boldsymbol{\eta}_t = \begin{pmatrix} \boldsymbol{\xi}_t' & \boldsymbol{\zeta}_t' & \boldsymbol{\omega}_t' & \mathbf{0}_{1\times 8} & \boldsymbol{e}_t' \end{pmatrix}',$$

$$\boldsymbol{\xi}_t = \begin{pmatrix} \xi_{t,y} \\ \xi_{t,x_1} \\ \xi_{t,x_2} \\ \xi_{t,x_3} \end{pmatrix}, \quad \boldsymbol{\zeta}_t = \begin{pmatrix} \zeta_{t,y} \\ \zeta_{t,x_1} \\ \zeta_{t,x_2} \\ \zeta_{t,x_3} \end{pmatrix}, \quad \boldsymbol{\omega}_t = \begin{pmatrix} \omega_{t,y} \\ \omega_{t,x_1} \\ \omega_{t,x_2} \\ \omega_{t,x_3} \end{pmatrix}, \quad \boldsymbol{e}_t = \begin{pmatrix} e_{t,1} \\ e_{t,2} \\ e_{t,3} \end{pmatrix}.$$

The covariance matrix of the disturbance terms is a blockdiagonal matrix of:

$$\boldsymbol{\Sigma}_{\eta} = \text{diag}(\boldsymbol{\Sigma}_{\xi}, \boldsymbol{\Sigma}_{\zeta}, \boldsymbol{\Sigma}_{\omega}, \mathbf{0}_{8\times 8}, \boldsymbol{\Sigma}_{e}), \tag{SA.16}$$

where,

$$\boldsymbol{\Sigma}_{e} = \begin{bmatrix} \sigma^2_e & 0 & 0 \\ 0 & \sigma^2_e & 0 \\ 0 & 0 & \sigma^2_e \end{bmatrix}, \tag{SA.17}$$

and it is expected that $\sigma^2_e = 1$ due to the scaling of the sampling error.

# References


Commandeur, J. J. F. and S. J. Koopman (2007). *An Introduction to State Space Time Series Analysis*. Oxford: Oxford University Press.

Durbin, J. and S. J. Koopman (2012). *Time Series Analysis by State Space Methods* (2nd ed.). Oxford: Oxford University Press.

Harvey, A. and S. Koopman (1997). *Multivariate structural time series models*, pp. 269–298. Series in Financial Economics and Quantitative Analysis. John Wiley & Sons. Pagination: 372.

Harvey, A. C. (1989). *Forecasting, structural time series models and the Kalman filter*. Cambridge: Cambridge University Press.

Koopman, S. J., A. C. Harvey, J. A. Doornik, and N. Shephard (2009). *Stamp 8.2: Structural Time Series Analyser, Modeller and Predictor*. London: Timberlake Consultants.

van den Brakel, J. and J. Michiels (2021). Nowcasting register labour force participation rates in municipal districts using survey data. *Journal of Official Statistics 37*(4), 1009–1045.

# SB Supplementary material Section 3

## SB.1 Tables

Table SB1: Parameter estimates.

| Model | 1 | 2 | 3 | 4 | 5 | 6 |
|---|---|---|---|---|---|---|
| $\hat{\sigma}^2_{\xi}$ | 0.0005 | 0.0005 | 0.0005 | 0.0005 | 0.0005 | 0.0005 |
| $\hat{\theta}_{\mu,2}$ | 1 | 1 | 1 | 1.2089 | 1.2747 | 1.2328 |
| $\hat{\theta}_{\mu,3}$ | 1 | 1 | 1 | 0.9900 | 0.9861 | 1.0910 |
| $\hat{\theta}_{\mu,4}$ | 1 | 1 | 1 | 0.9466 | 0.9358 | 0.9253 |
| $\hat{\sigma}^2_{\zeta}$ | - | 2.574e-14 | 9.896e-13 | - | 1.754e-08 | 1.586e-12 |
| $\hat{\theta}_{\nu,2}$ | - | 1 | -180.2032 | - | 1 | 90.7448 |
| $\hat{\theta}_{\nu,3}$ | - | 1 | 57.4598 | - | 1 | -151.8539 |
| $\hat{\theta}_{\nu,4}$ | - | 1 | 74.5109 | - | 1 | -10.3725 |
| $\hat{\sigma}^2_{\omega}$ | - | 2.519e-06 | 0 | - | 2.570e-06 | 2.822e-06 |
| $\hat{\theta}_{\gamma,2}$ | - | 1 | 94.9402 | - | 1 | 0.9037 |
| $\hat{\theta}_{\gamma,3}$ | - | 1 | 101.0762 | - | 1 | 0.9014 |
| $\hat{\theta}_{\gamma,4}$ | - | 1 | -38.0955 | - | 1 | 0.9857 |
| $\hat{\sigma}^2_{\varepsilon_1}$ | 0.0199 | 0.0187 | 0.0198 | 0.0199 | 0.0189 | 0.0188 |
| $\hat{\sigma}^2_{\varepsilon_2}$ | 0.0239 | 0.0227 | 0.0233 | 0.0226 | 0.0216 | 0.0215 |
| $\hat{\sigma}^2_{\varepsilon_3}$ | 0.0220 | 0.0209 | 0.0220 | 0.0220 | 0.0211 | 0.0205 |
| $\hat{\sigma}^2_{\varepsilon_4}$ | 0.0216 | 0.0204 | 0.0215 | 0.0217 | 0.0209 | 0.0206 |
| $\hat{\rho}_{\varepsilon_{2,1}}$ | 0.9282 | 0.9244 | 0.9364 | 0.9349 | 0.9335 | 0.9345 |
| $\hat{\rho}_{\varepsilon_{3,1}}$ | 0.8651 | 0.8577 | 0.8660 | 0.8651 | 0.8592 | 0.8617 |
| $\hat{\rho}_{\varepsilon_{4,1}}$ | 0.9020 | 0.8963 | 0.9038 | 0.9038 | 0.8994 | 0.8991 |
| $\hat{\rho}_{\varepsilon_{3,2}}$ | 0.8145 | 0.8050 | 0.8294 | 0.8226 | 0.8166 | 0.8190 |
| $\hat{\rho}_{\varepsilon_{4,2}}$ | 0.8377 | 0.8292 | 0.8552 | 0.8512 | 0.8464 | 0.8479 |
| $\hat{\rho}_{\varepsilon_{4,3}}$ | 0.9507 | 0.9480 | 0.9507 | 0.9510 | 0.9490 | 0.9509 |

Table SB2: Ljung-Box test statistics for different lag sizes. Test statistic is asymptotically chi-square distributed with df: lag size - (# parameters/$N$) - 1. Note that $N = 4$ and at $\alpha = 0.05$, none of the test statistics fall in the critical region (same holds at the 10% level).

| Model | | | | 1 | 2 | 3 | 4 | 5 | 6 |
|---|---|---|---|---|---|---|---|---|---|
| Series | lag size | lowest df | crit. value | | | | | | |
| $y_{1,t}$ | 40 | 34 | 48.602 | 32.011 | 31.503 | 32.269 | 30.111 | 31.061 | 32.158 |
| | 60 | 54 | 72.153 | 51.385 | 50.097 | 51.222 | 50.741 | 49.761 | 51.674 |
| | 80 | 74 | 95.081 | 66.249 | 68.169 | 66.202 | 64.280 | 65.647 | 68.152 |
| | 100 | 94 | 117.632 | 82.223 | 83.624 | 82.387 | 79.641 | 80.169 | 83.859 |
| | 120 | 114 | 139.921 | 101.333 | 101.303 | 101.448 | 101.365 | 100.938 | 103.756 |
| $y_{2,t}$ | 40 | 34 | 48.602 | 35.462 | 36.568 | 30.785 | 29.617 | 31.716 | 29.703 |
| | 60 | 54 | 72.153 | 47.955 | 48.162 | 43.374 | 43.035 | 44.219 | 42.180 |
| | 80 | 74 | 95.081 | 68.466 | 71.632 | 64.542 | 64.190 | 67.483 | 65.940 |
| | 100 | 94 | 117.632 | 85.215 | 86.953 | 81.537 | 82.119 | 83.791 | 82.998 |
| | 120 | 114 | 139.921 | 95.300 | 96.092 | 90.259 | 91.174 | 91.695 | 91.676 |
| $y_{3,t}$ | 40 | 34 | 48.602 | 38.912 | 39.618 | 38.296 | 36.158 | 39.944 | 37.518 |
| | 60 | 54 | 72.153 | 52.676 | 51.860 | 52.310 | 49.401 | 51.199 | 50.681 |
| | 80 | 74 | 95.081 | 69.193 | 70.087 | 68.842 | 64.097 | 67.175 | 65.907 |
| | 100 | 94 | 117.632 | 85.640 | 87.547 | 85.443 | 78.052 | 81.823 | 82.163 |
| | 120 | 114 | 139.921 | 114.088 | 113.757 | 113.842 | 105.179 | 108.291 | 107.291 |
| $y_{4,t}$ | 40 | 34 | 48.602 | 31.202 | 35.616 | 30.615 | 27.135 | 33.013 | 34.679 |
| | 60 | 54 | 72.153 | 57.706 | 61.164 | 57.248 | 55.261 | 59.677 | 62.875 |
| | 80 | 74 | 95.081 | 72.031 | 76.367 | 71.755 | 67.363 | 72.496 | 75.598 |
| | 100 | 94 | 117.632 | 90.964 | 95.691 | 90.971 | 85.589 | 90.668 | 95.386 |
| | 120 | 114 | 139.921 | 108.716 | 111.944 | 108.741 | 104.074 | 107.436 | 112.104 |
| # parameters | | | | 11 | 13 | 19 | 14 | 16 | 22 |

Table SB3: MSE forecasting performance based on the 1- to 12-step ahead forecasts per forecasting year and in total relative to the MSE of the univariate benchmark (DBSTS).

| Scenario | Model | 2011 | 2012 | 2013 | 2014 | 2015 | 2016 | 2017 | 2018 | 2019 | 2020 | 2021 | 2022 | Total |
|---|---|---|---|---|---|---|---|---|---|---|---|---|---|---|
| 1 | DBSTS | 1.000 | 1.000 | 1.000 | 1.000 | 1.000 | 1.000 | 1.000 | 1.000 | 1.000 | 1.000 | 1.000 | 1.000 | 1.000 |
| | SBSTS | 1.033 | 1.000 | 1.000 | 1.000 | 1.000 | 1.000 | 1.000 | 1.000 | 1.000 | 1.000 | 1.000 | 1.000 | 1.003 |
| 2 | 1 | 0.963 | 0.911 | 1.178 | 1.045 | 0.846 | 0.931 | 0.930 | 0.993 | 1.074 | 0.942 | 1.090 | 0.970 | 0.998 |
| | 2 | 1.032 | 0.929 | 1.079 | 1.015 | 0.980 | 1.030 | 1.039 | 1.000 | 1.075 | 1.020 | 1.044 | 0.950 | 1.012 |
| | 3 | 1.004 | 0.880 | 0.969 | 1.113 | 0.916 | 1.086 | 1.333 | 1.018 | 1.149 | 0.968 | 1.063 | 0.950 | 1.015 |
| | 4 | 1.182 | 1.016 | 1.051 | 1.054 | 1.019 | 1.000 | 0.946 | 0.905 | 0.872 | 1.082 | 1.066 | 1.072 | 1.034 |
| | 5 | 1.046 | 1.039 | 1.028 | 1.024 | 0.963 | 1.106 | 1.028 | 0.771 | 0.785 | 1.564 | 1.255 | 0.848 | 1.015 |
| | 6 | 1.156 | 1.563 | 0.905 | 1.112 | 1.109 | 1.198 | 1.716 | 1.112 | 1.927 | 0.856 | 1.041 | 1.341 | 1.191 |
| 3 | 1 | 0.695 | 0.815 | 0.280 | 0.367 | 0.638 | 0.473 | 0.878 | 0.700 | 1.339 | 1.194 | 0.601 | 0.242 | 0.569 |
| | 2 | 0.774 | 0.829 | 0.245 | 0.483 | 0.598 | 0.473 | 0.926 | 0.677 | 1.278 | 1.283 | 0.599 | 0.223 | 0.574 |
| | 3 | 0.736 | 0.731 | 0.234 | 0.490 | 0.642 | 0.470 | 1.053 | 0.585 | 1.133 | 1.396 | 0.637 | 0.302 | 0.581 |
| | 4 | 0.745 | 0.662 | 0.293 | 0.294 | 0.796 | 0.534 | 0.955 | 0.654 | 1.154 | 1.370 | 0.648 | 0.244 | 0.588 |
| | 5 | 0.771 | 0.663 | 0.263 | 0.334 | 0.712 | 0.486 | 0.957 | 0.650 | 1.376 | 1.448 | 0.552 | 0.358 | 0.597 |
| | 6 | 0.876 | 0.886 | 0.228 | 0.443 | 0.775 | 0.433 | 1.029 | 0.494 | 1.131 | 1.893 | 0.682 | 0.422 | 0.643 |
| 4 | 1 | 0.538 | 0.422 | 0.194 | 0.366 | 0.308 | 0.210 | 0.554 | 0.248 | 1.308 | 1.166 | 0.454 | 0.090 | 0.364 |
| | 2 | 0.603 | 0.418 | 0.183 | 0.379 | 0.294 | 0.197 | 0.607 | 0.243 | 1.260 | 1.232 | 0.479 | 0.085 | 0.372 |
| | 3 | 2.400 | 3.143 | 0.344 | 0.410 | 0.579 | 0.544 | 0.604 | 0.796 | 1.752 | 2.131 | 1.572 | 0.163 | 1.003 |
| | 4 | 0.534 | 0.309 | 0.196 | 0.342 | 0.423 | 0.233 | 0.607 | 0.236 | 1.156 | 1.340 | 0.467 | 0.097 | 0.375 |
| | 5 | 0.636 | 0.330 | 0.179 | 0.370 | 0.398 | 0.219 | 0.677 | 0.237 | 1.085 | 1.639 | 0.471 | 0.048 | 0.388 |
| | 6 | 0.598 | 0.327 | 0.174 | 0.421 | 0.321 | 0.194 | 0.719 | 0.214 | 1.107 | 1.738 | 0.538 | 0.069 | 0.394 |
| 5 | 1 | 0.068 | 0.162 | 0.031 | 0.151 | 0.047 | 0.091 | 0.118 | 0.049 | 0.300 | 0.105 | 0.139 | 0.013 | 0.080 |
| | 2 | 0.070 | 0.160 | 0.030 | 0.150 | 0.045 | 0.090 | 0.118 | 0.049 | 0.301 | 0.106 | 0.140 | 0.013 | 0.079 |
| | 3 | 0.074 | 0.279 | 0.034 | 0.204 | 0.126 | 0.142 | 0.328 | 0.113 | 0.605 | 0.116 | 0.197 | 0.130 | 0.152 |
| | 4 | 0.029 | 0.150 | 0.030 | 0.144 | 0.090 | 0.145 | 0.191 | 0.099 | 0.586 | 0.327 | 0.117 | 0.143 | 0.131 |
| | 5 | 0.029 | 0.183 | 0.029 | 0.146 | 0.058 | 0.095 | 0.109 | 0.039 | 0.253 | 0.098 | 0.140 | 0.012 | 0.074 |
| | 6 | 0.070 | 0.197 | 0.023 | 0.154 | 0.041 | 0.084 | 0.171 | 0.046 | 0.259 | 0.133 | 0.165 | 0.019 | 0.086 |

Table SB4: MSE forecasting performance based on the 1- to 12-step ahead forecasts per month, averaged over the years 2011-2022.

| Scenario | Model | Jan $t+1$ | Feb $t+2$ | Mar $t+3$ | Apr $t+4$ | May $t+5$ | June $t+6$ | July $t+7$ | Aug $t+8$ | Sept $t+9$ | Oct $t+10$ | Nov $t+11$ | Dec $t+12$ |
|---|---|---|---|---|---|---|---|---|---|---|---|---|---|
| 1 | DBSTS | 1.000 | 1.000 | 1.000 | 1.000 | 1.000 | 1.000 | 1.000 | 1.000 | 1.000 | 1.000 | 1.000 | 1.000 |
| | SBSTS | 0.998 | 0.997 | 0.997 | 1.008 | 0.999 | 1.004 | 0.999 | 1.001 | 1.011 | 0.999 | 0.996 | 1.025 |
| 2 | 1 | 1.213 | 1.006 | 0.909 | 0.933 | 1.055 | 1.015 | 0.969 | 0.942 | 1.057 | 0.951 | 1.035 | 0.883 |
| | 2 | 1.133 | 1.068 | 0.895 | 1.006 | 1.046 | 1.047 | 0.967 | 0.968 | 1.039 | 0.974 | 1.009 | 0.971 |
| | 3 | 1.044 | 1.074 | 1.001 | 0.990 | 1.100 | 1.054 | 0.994 | 0.985 | 1.026 | 0.940 | 1.158 | 0.960 |
| | 4 | 1.056 | 0.961 | 1.041 | 1.005 | 1.169 | 0.964 | 0.977 | 1.078 | 1.131 | 1.001 | 1.030 | 1.126 |
| | 5 | 1.215 | 1.181 | 0.970 | 1.030 | 0.942 | 0.824 | 0.863 | 1.007 | 0.926 | 1.079 | 0.829 | 1.018 |
| | 6 | 0.954 | 1.078 | 1.550 | 1.171 | 1.315 | 1.261 | 1.198 | 1.469 | 1.173 | 1.045 | 1.029 | 1.362 |
| 3 | 1 | 0.132 | 0.240 | 0.226 | 0.111 | 0.242 | 0.505 | 0.817 | 0.692 | 0.911 | 0.903 | 1.082 | 0.892 |
| | 2 | 0.117 | 0.245 | 0.225 | 0.113 | 0.228 | 0.510 | 0.803 | 0.689 | 0.898 | 0.909 | 1.139 | 0.962 |
| | 3 | 0.114 | 0.259 | 0.236 | 0.141 | 0.197 | 0.467 | 0.813 | 0.821 | 0.833 | 0.921 | 1.204 | 0.916 |
| | 4 | 0.106 | 0.271 | 0.231 | 0.173 | 0.288 | 0.445 | 0.816 | 0.779 | 0.886 | 0.930 | 1.002 | 1.015 |
| | 5 | 0.111 | 0.275 | 0.281 | 0.159 | 0.278 | 0.614 | 0.782 | 0.843 | 0.859 | 0.990 | 0.904 | 0.939 |
| | 6 | 0.107 | 0.281 | 0.273 | 0.243 | 0.237 | 0.509 | 0.784 | 1.088 | 0.846 | 1.000 | 1.132 | 1.158 |
| 4 | 1 | 0.135 | 0.246 | 0.223 | 0.112 | 0.234 | 0.506 | 0.153 | 0.200 | 0.112 | 0.767 | 1.219 | 0.783 |
| | 2 | 0.119 | 0.251 | 0.223 | 0.114 | 0.222 | 0.511 | 0.156 | 0.202 | 0.108 | 0.786 | 1.208 | 0.860 |
| | 3 | 0.233 | 0.318 | 0.522 | 0.403 | 1.679 | 1.273 | 0.861 | 0.787 | 1.906 | 1.175 | 2.936 | 1.744 |
| | 4 | 0.119 | 0.270 | 0.221 | 0.153 | 0.300 | 0.421 | 0.153 | 0.195 | 0.111 | 0.803 | 1.127 | 0.891 |
| | 5 | 0.121 | 0.281 | 0.233 | 0.136 | 0.248 | 0.448 | 0.170 | 0.223 | 0.095 | 0.930 | 0.992 | 0.883 |
| | 6 | 0.120 | 0.271 | 0.231 | 0.173 | 0.208 | 0.425 | 0.158 | 0.313 | 0.088 | 0.877 | 1.281 | 0.838 |
| 5 | 1 | 0.052 | 0.045 | 0.107 | 0.134 | 0.261 | 0.173 | 0.053 | 0.081 | 0.018 | 0.039 | 0.219 | 0.044 |
| | 2 | 0.049 | 0.045 | 0.109 | 0.134 | 0.258 | 0.173 | 0.054 | 0.081 | 0.018 | 0.039 | 0.216 | 0.045 |
| | 3 | 0.092 | 0.069 | 0.161 | 0.198 | 0.381 | 0.350 | 0.084 | 0.223 | 0.054 | 0.077 | 0.488 | 0.139 |
| | 4 | 0.040 | 0.079 | 0.125 | 0.158 | 0.472 | 0.316 | 0.072 | 0.161 | 0.117 | 0.069 | 0.337 | 0.105 |
| | 5 | 0.041 | 0.058 | 0.105 | 0.107 | 0.304 | 0.173 | 0.047 | 0.086 | 0.027 | 0.026 | 0.173 | 0.029 |
| | 6 | 0.046 | 0.055 | 0.116 | 0.125 | 0.308 | 0.223 | 0.053 | 0.090 | 0.025 | 0.039 | 0.218 | 0.042 |

Table SB5: MAPE forecasting performance based on the 1- to 12-step ahead forecasts per forecasting year and in total relative to the MAPE of the univariate benchmark (DBSTS).

| Scenario | Model | 2011 | 2012 | 2013 | 2014 | 2015 | 2016 | 2017 | 2018 | 2019 | 2020 | 2021 | 2022 | Total |
|---|---|---|---|---|---|---|---|---|---|---|---|---|---|---|
| 1 | DBSTS | 1.000 | 1.000 | 1.000 | 1.000 | 1.000 | 1.000 | 1.000 | 1.000 | 1.000 | 1.000 | 1.000 | 1.000 | 1.000 |
| | SBSTS | 0.994 | 1.000 | 1.000 | 1.000 | 1.000 | 1.000 | 1.000 | 1.000 | 1.000 | 1.000 | 1.000 | 1.000 | 1.000 |
| 2 | 1 | 1.028 | 1.018 | 1.084 | 1.098 | 0.908 | 0.943 | 0.934 | 0.984 | 1.051 | 0.991 | 1.026 | 0.967 | 1.001 |
| | 2 | 1.015 | 0.996 | 1.047 | 1.007 | 1.008 | 0.984 | 1.023 | 0.993 | 1.035 | 1.016 | 1.015 | 0.975 | 1.008 |
| | 3 | 1.049 | 0.985 | 0.987 | 1.047 | 0.981 | 1.014 | 1.184 | 0.993 | 1.077 | 0.988 | 1.046 | 0.982 | 1.022 |
| | 4 | 1.051 | 0.994 | 1.009 | 1.041 | 1.020 | 0.980 | 0.946 | 0.943 | 0.963 | 1.068 | 1.028 | 1.039 | 1.006 |
| | 5 | 1.014 | 1.030 | 1.011 | 0.998 | 0.999 | 1.011 | 0.991 | 0.881 | 0.896 | 1.311 | 1.157 | 0.897 | 1.005 |
| | 6 | 1.021 | 1.223 | 0.951 | 0.993 | 1.072 | 1.123 | 1.253 | 1.041 | 1.396 | 1.101 | 0.995 | 1.214 | 1.102 |
| 3 | 1 | 0.666 | 0.960 | 0.454 | 0.729 | 0.679 | 0.733 | 0.874 | 0.715 | 1.173 | 1.219 | 0.782 | 0.387 | 0.726 |
| | 2 | 0.682 | 0.963 | 0.414 | 0.841 | 0.676 | 0.701 | 0.885 | 0.707 | 1.136 | 1.272 | 0.775 | 0.364 | 0.724 |
| | 3 | 0.751 | 0.893 | 0.379 | 0.826 | 0.720 | 0.676 | 0.932 | 0.649 | 1.066 | 1.417 | 0.802 | 0.408 | 0.730 |
| | 4 | 0.674 | 0.880 | 0.424 | 0.677 | 0.800 | 0.773 | 0.908 | 0.692 | 1.104 | 1.352 | 0.798 | 0.389 | 0.733 |
| | 5 | 0.714 | 0.858 | 0.417 | 0.723 | 0.747 | 0.725 | 0.887 | 0.706 | 1.165 | 1.289 | 0.781 | 0.439 | 0.732 |
| | 6 | 0.707 | 0.952 | 0.390 | 0.803 | 0.829 | 0.651 | 0.908 | 0.623 | 1.025 | 1.673 | 0.833 | 0.472 | 0.756 |
| 4 | 1 | 0.652 | 0.704 | 0.366 | 0.743 | 0.409 | 0.528 | 0.713 | 0.479 | 1.143 | 1.170 | 0.722 | 0.248 | 0.593 |
| | 2 | 0.658 | 0.700 | 0.340 | 0.758 | 0.392 | 0.487 | 0.721 | 0.477 | 1.111 | 1.215 | 0.727 | 0.248 | 0.588 |
| | 3 | 1.810 | 2.018 | 0.628 | 0.795 | 0.706 | 0.912 | 0.654 | 0.842 | 1.252 | 1.852 | 1.242 | 0.405 | 1.012 |
| | 4 | 0.638 | 0.493 | 0.335 | 0.690 | 0.498 | 0.576 | 0.749 | 0.463 | 1.109 | 1.341 | 0.727 | 0.258 | 0.592 |
| | 5 | 0.683 | 0.577 | 0.312 | 0.734 | 0.477 | 0.536 | 0.735 | 0.475 | 1.057 | 1.466 | 0.720 | 0.201 | 0.593 |
| | 6 | 0.709 | 0.530 | 0.308 | 0.758 | 0.447 | 0.447 | 0.751 | 0.450 | 1.048 | 1.557 | 0.768 | 0.248 | 0.596 |
| 5 | 1 | 0.306 | 0.419 | 0.161 | 0.452 | 0.181 | 0.385 | 0.310 | 0.197 | 0.503 | 0.374 | 0.400 | 0.117 | 0.290 |
| | 2 | 0.312 | 0.416 | 0.155 | 0.445 | 0.182 | 0.379 | 0.310 | 0.195 | 0.505 | 0.373 | 0.401 | 0.116 | 0.289 |
| | 3 | 0.289 | 0.548 | 0.175 | 0.521 | 0.335 | 0.451 | 0.552 | 0.322 | 0.750 | 0.447 | 0.492 | 0.355 | 0.409 |
| | 4 | 0.211 | 0.394 | 0.164 | 0.440 | 0.274 | 0.440 | 0.404 | 0.293 | 0.766 | 0.734 | 0.393 | 0.420 | 0.381 |
| | 5 | 0.215 | 0.446 | 0.154 | 0.448 | 0.214 | 0.401 | 0.319 | 0.193 | 0.494 | 0.347 | 0.401 | 0.111 | 0.286 |
| | 6 | 0.354 | 0.469 | 0.148 | 0.419 | 0.192 | 0.367 | 0.353 | 0.204 | 0.509 | 0.438 | 0.430 | 0.144 | 0.307 |

Table SB6: MAE forecasting performance based on the 1- to 12-step ahead forecasts per forecasting year and in total relative to the MAE of the univariate benchmark (DBSTS).

| Scenario | Model | 2011 | 2012 | 2013 | 2014 | 2015 | 2016 | 2017 | 2018 | 2019 | 2020 | 2021 | 2022 | Total |
|---|---|---|---|---|---|---|---|---|---|---|---|---|---|---|
| 1 | DBSTS | 1.000 | 1.000 | 1.000 | 1.000 | 1.000 | 1.000 | 1.000 | 1.000 | 1.000 | 1.000 | 1.000 | 1.000 | 1.000 |
| | SBSTS | 0.996 | 1.000 | 1.000 | 1.000 | 1.000 | 1.000 | 1.000 | 1.000 | 1.000 | 1.000 | 1.000 | 1.000 | 1.000 |
| 2 | 1 | 1.020 | 1.012 | 1.079 | 1.089 | 0.910 | 0.943 | 0.934 | 0.986 | 1.052 | 0.994 | 1.022 | 0.969 | 0.998 |
| | 2 | 1.014 | 0.993 | 1.043 | 1.010 | 1.005 | 0.984 | 1.020 | 0.994 | 1.036 | 1.019 | 1.014 | 0.975 | 1.006 |
| | 3 | 1.042 | 0.981 | 0.986 | 1.052 | 0.975 | 1.014 | 1.180 | 0.993 | 1.078 | 0.990 | 1.048 | 0.981 | 1.020 |
| | 4 | 1.061 | 0.997 | 1.007 | 1.040 | 1.020 | 0.981 | 0.946 | 0.942 | 0.961 | 1.063 | 1.036 | 1.039 | 1.007 |
| | 5 | 1.014 | 1.030 | 1.009 | 1.003 | 0.996 | 1.012 | 0.986 | 0.875 | 0.887 | 1.304 | 1.138 | 0.899 | 0.999 |
| | 6 | 1.026 | 1.232 | 0.962 | 1.002 | 1.071 | 1.125 | 1.262 | 1.044 | 1.400 | 1.120 | 1.005 | 1.208 | 1.110 |
| 3 | 1 | 0.685 | 0.942 | 0.489 | 0.713 | 0.687 | 0.731 | 0.879 | 0.728 | 1.167 | 1.221 | 0.823 | 0.390 | 0.734 |
| | 2 | 0.702 | 0.946 | 0.447 | 0.823 | 0.682 | 0.700 | 0.889 | 0.719 | 1.130 | 1.275 | 0.816 | 0.367 | 0.732 |
| | 3 | 0.763 | 0.879 | 0.415 | 0.810 | 0.724 | 0.676 | 0.935 | 0.657 | 1.059 | 1.417 | 0.845 | 0.413 | 0.737 |
| | 4 | 0.692 | 0.876 | 0.462 | 0.664 | 0.806 | 0.773 | 0.915 | 0.704 | 1.095 | 1.351 | 0.842 | 0.391 | 0.742 |
| | 5 | 0.729 | 0.849 | 0.453 | 0.708 | 0.754 | 0.725 | 0.891 | 0.718 | 1.154 | 1.293 | 0.816 | 0.446 | 0.741 |
| | 6 | 0.726 | 0.956 | 0.424 | 0.790 | 0.831 | 0.649 | 0.908 | 0.625 | 1.009 | 1.676 | 0.877 | 0.480 | 0.764 |
| 4 | 1 | 0.659 | 0.694 | 0.391 | 0.730 | 0.413 | 0.517 | 0.706 | 0.473 | 1.135 | 1.171 | 0.751 | 0.236 | 0.591 |
| | 2 | 0.668 | 0.689 | 0.366 | 0.746 | 0.396 | 0.477 | 0.714 | 0.471 | 1.104 | 1.217 | 0.757 | 0.237 | 0.587 |
| | 3 | 1.818 | 1.979 | 0.648 | 0.785 | 0.710 | 0.874 | 0.645 | 0.853 | 1.251 | 1.859 | 1.330 | 0.405 | 1.016 |
| | 4 | 0.646 | 0.492 | 0.363 | 0.680 | 0.501 | 0.567 | 0.743 | 0.455 | 1.098 | 1.342 | 0.756 | 0.246 | 0.591 |
| | 5 | 0.688 | 0.572 | 0.340 | 0.723 | 0.480 | 0.527 | 0.727 | 0.468 | 1.044 | 1.466 | 0.746 | 0.196 | 0.591 |
| | 6 | 0.714 | 0.527 | 0.336 | 0.746 | 0.447 | 0.440 | 0.742 | 0.437 | 1.032 | 1.557 | 0.797 | 0.240 | 0.593 |
| 5 | 1 | 0.300 | 0.410 | 0.171 | 0.450 | 0.177 | 0.374 | 0.305 | 0.196 | 0.493 | 0.386 | 0.409 | 0.113 | 0.288 |
| | 2 | 0.306 | 0.407 | 0.165 | 0.444 | 0.178 | 0.369 | 0.305 | 0.194 | 0.495 | 0.385 | 0.410 | 0.113 | 0.287 |
| | 3 | 0.283 | 0.533 | 0.183 | 0.512 | 0.331 | 0.435 | 0.542 | 0.317 | 0.737 | 0.463 | 0.508 | 0.355 | 0.407 |
| | 4 | 0.201 | 0.387 | 0.174 | 0.438 | 0.270 | 0.431 | 0.407 | 0.290 | 0.765 | 0.759 | 0.406 | 0.410 | 0.381 |
| | 5 | 0.206 | 0.435 | 0.164 | 0.445 | 0.211 | 0.391 | 0.318 | 0.191 | 0.487 | 0.360 | 0.410 | 0.108 | 0.284 |
| | 6 | 0.345 | 0.457 | 0.155 | 0.419 | 0.187 | 0.358 | 0.346 | 0.203 | 0.502 | 0.453 | 0.443 | 0.141 | 0.305 |

Table SB7: Quantiles of forecast errors over the entire real time window relative to the error of the benchmark (DBSTS).

| | | Quantiles | | | | | | | | | | |
|---|---|---|---|---|---|---|---|---|---|---|---|---|
| Scenario | Model | 0.01 | 0.025 | 0.05 | 0.1 | 0.25 | 0.5 | 0.75 | 0.9 | 0.95 | 0.975 | 0.99 |
| 1 | DBSTS | 1.000 | 1.000 | 1.000 | 1.000 | 1.000 | 1.000 | 1.000 | 1.000 | 1.000 | 1.000 | 1.000 |
| | SBSTS | 1.000 | 1.000 | 1.000 | 1.000 | 1.000 | 1.000 | 1.000 | 1.014 | 1.000 | 1.000 | 1.002 |
| 2 | 1 | 1.044 | 1.092 | 1.041 | 1.121 | 1.414 | 0.558 | 0.958 | 0.973 | 0.950 | 0.997 | 0.955 |
| | 2 | 1.026 | 1.069 | 1.052 | 1.029 | 1.162 | 0.845 | 0.987 | 0.998 | 0.936 | 1.003 | 1.013 |
| | 3 | 1.005 | 1.055 | 1.120 | 1.080 | 1.229 | 0.744 | 0.996 | 1.010 | 0.949 | 0.990 | 0.998 |
| | 4 | 1.033 | 0.979 | 1.008 | 0.855 | 1.156 | 0.912 | 0.947 | 1.132 | 0.991 | 0.999 | 1.020 |
| | 5 | 1.194 | 1.099 | 1.237 | 1.067 | 1.581 | 0.466 | 0.920 | 0.963 | 0.927 | 0.957 | 1.003 |
| | 6 | 0.907 | 0.864 | 0.730 | 0.741 | 0.324 | 1.865 | 1.254 | 1.226 | 1.050 | 1.066 | 1.082 |
| 3 | 1 | 0.515 | 0.686 | 0.759 | 0.812 | 1.078 | 0.335 | 0.604 | 0.742 | 0.825 | 0.825 | 0.771 |
| | 2 | 0.523 | 0.741 | 0.832 | 0.822 | 1.075 | 0.390 | 0.579 | 0.742 | 0.802 | 0.866 | 0.766 |
| | 3 | 0.542 | 0.712 | 0.891 | 0.808 | 1.442 | 0.092 | 0.666 | 0.731 | 0.789 | 0.872 | 0.793 |
| | 4 | 0.426 | 0.546 | 0.739 | 0.722 | 1.083 | 0.532 | 0.777 | 0.799 | 0.840 | 0.873 | 0.758 |
| | 5 | 0.495 | 0.634 | 0.830 | 0.768 | 0.863 | 0.446 | 0.606 | 0.799 | 0.808 | 0.845 | 0.813 |
| | 6 | 0.610 | 0.650 | 0.852 | 0.763 | 1.165 | 0.313 | 0.633 | 0.885 | 0.781 | 0.799 | 0.858 |
| 4 | 1 | 0.452 | 0.627 | 0.796 | 0.861 | 1.374 | -0.129 | 0.401 | 0.528 | 0.507 | 0.611 | 0.602 |
| | 2 | 0.485 | 0.617 | 0.784 | 0.836 | 1.312 | -0.111 | 0.368 | 0.525 | 0.503 | 0.608 | 0.630 |
| | 3 | 0.913 | 1.159 | 1.298 | 1.175 | 2.081 | 0.088 | 0.736 | 0.912 | 0.879 | 0.905 | 1.040 |
| | 4 | 0.439 | 0.624 | 0.785 | 0.789 | 1.242 | 0.046 | 0.419 | 0.548 | 0.489 | 0.611 | 0.639 |
| | 5 | 0.546 | 0.633 | 0.785 | 0.801 | 1.227 | -0.051 | 0.401 | 0.514 | 0.491 | 0.610 | 0.615 |
| | 6 | 0.594 | 0.660 | 0.870 | 0.924 | 1.424 | 0.021 | 0.387 | 0.438 | 0.450 | 0.585 | 0.625 |
| 5 | 1 | 0.273 | 0.384 | 0.486 | 0.525 | 0.822 | -0.097 | 0.150 | 0.233 | 0.218 | 0.209 | 0.193 |
| | 2 | 0.275 | 0.382 | 0.488 | 0.520 | 0.847 | -0.098 | 0.151 | 0.232 | 0.223 | 0.211 | 0.190 |
| | 3 | 0.351 | 0.516 | 0.676 | 0.736 | 1.345 | -0.374 | 0.170 | 0.269 | 0.228 | 0.247 | 0.295 |
| | 4 | 0.242 | 0.331 | 0.350 | 0.245 | 0.218 | 0.549 | 0.457 | 0.417 | 0.341 | 0.339 | 0.313 |
| | 5 | 0.272 | 0.395 | 0.509 | 0.392 | 0.697 | -0.002 | 0.185 | 0.226 | 0.224 | 0.224 | 0.225 |
| | 6 | 0.286 | 0.425 | 0.548 | 0.501 | 0.668 | 0.072 | 0.224 | 0.229 | 0.217 | 0.217 | 0.197 |

Table SB8: Real-time hyperparameter estimates of model 4 in forecast scenario 3.

| | 2011 | 2012 | 2013 | 2014 | 2015 | 2016 | 2017 | 2018 | 2019 | 2020 | 2021 | 2022 |
|---|---|---|---|---|---|---|---|---|---|---|---|---|
| $\hat{\sigma}^2_{\xi}$ | 0.0002 | 0.0002 | 0.0002 | 0.0001 | 0.0001 | 0.0002 | 0.0002 | 0.0002 | 0.0003 | 0.0003 | 0.0003 | 0.0005 |
| $\hat{\theta}_{\mu,2}$ | 1.2646 | 1.3993 | 1.4644 | 1.4910 | 1.4967 | 1.3865 | 1.2426 | 1.2558 | 1.2419 | 1.2379 | 1.2159 | 1.2073 |
| $\hat{\theta}_{\mu,3}$ | 1.9184 | 2.1501 | 1.6638 | 1.6446 | 1.5516 | 1.2046 | 1.1237 | 0.9525 | 0.9069 | 0.8985 | 0.9137 | 0.9676 |
| $\hat{\theta}_{\mu,4}$ | 1.0381 | 1.0632 | 0.9874 | 0.9513 | 0.9646 | 0.9343 | 0.9055 | 0.8808 | 0.8841 | 0.8700 | 0.8951 | 0.9429 |
| $\hat{\sigma}^2_{\varepsilon_1}$ | 0.0170 | 0.0177 | 0.0192 | 0.0198 | 0.0196 | 0.0194 | 0.0196 | 0.0196 | 0.0198 | 0.0194 | 0.0196 | 0.0199 |
| $\hat{\sigma}^2_{\varepsilon_2}$ | 0.0197 | 0.0204 | 0.0215 | 0.0223 | 0.0217 | 0.0214 | 0.0223 | 0.0220 | 0.0224 | 0.0219 | 0.0225 | 0.0226 |
| $\hat{\sigma}^2_{\varepsilon_3}$ | 0.0165 | 0.0174 | 0.0205 | 0.0216 | 0.0211 | 0.0209 | 0.0205 | 0.0213 | 0.0216 | 0.0214 | 0.0219 | 0.0217 |
| $\hat{\sigma}^2_{\varepsilon_4}$ | 0.0197 | 0.0194 | 0.0216 | 0.0228 | 0.0225 | 0.0223 | 0.0219 | 0.0219 | 0.0218 | 0.0213 | 0.0217 | 0.0212 |
| $\hat{\rho}_{\varepsilon_{2,1}}$ | 0.9463 | 0.9468 | 0.9486 | 0.9484 | 0.9456 | 0.9437 | 0.9398 | 0.9391 | 0.9409 | 0.9373 | 0.9376 | 0.9347 |
| $\hat{\rho}_{\varepsilon_{3,1}}$ | 0.8674 | 0.8845 | 0.8925 | 0.9012 | 0.8848 | 0.8855 | 0.8809 | 0.8824 | 0.8798 | 0.8700 | 0.8678 | 0.8608 |
| $\hat{\rho}_{\varepsilon_{4,1}}$ | 0.9303 | 0.9292 | 0.9310 | 0.9320 | 0.9287 | 0.9196 | 0.9179 | 0.9121 | 0.9125 | 0.9063 | 0.9053 | 0.9027 |
| $\hat{\rho}_{\varepsilon_{3,2}}$ | 0.8232 | 0.8364 | 0.8492 | 0.8562 | 0.8404 | 0.8378 | 0.8395 | 0.8401 | 0.8424 | 0.8280 | 0.8258 | 0.8198 |
| $\hat{\rho}_{\varepsilon_{4,2}}$ | 0.8944 | 0.8907 | 0.8938 | 0.8943 | 0.8887 | 0.8771 | 0.8751 | 0.8691 | 0.8725 | 0.8624 | 0.8584 | 0.8507 |
| $\hat{\rho}_{\varepsilon_{4,3}}$ | 0.9330 | 0.9420 | 0.9506 | 0.9497 | 0.9494 | 0.9546 | 0.9538 | 0.9510 | 0.9497 | 0.9506 | 0.9524 | 0.9494 |

## SB.2 Figures

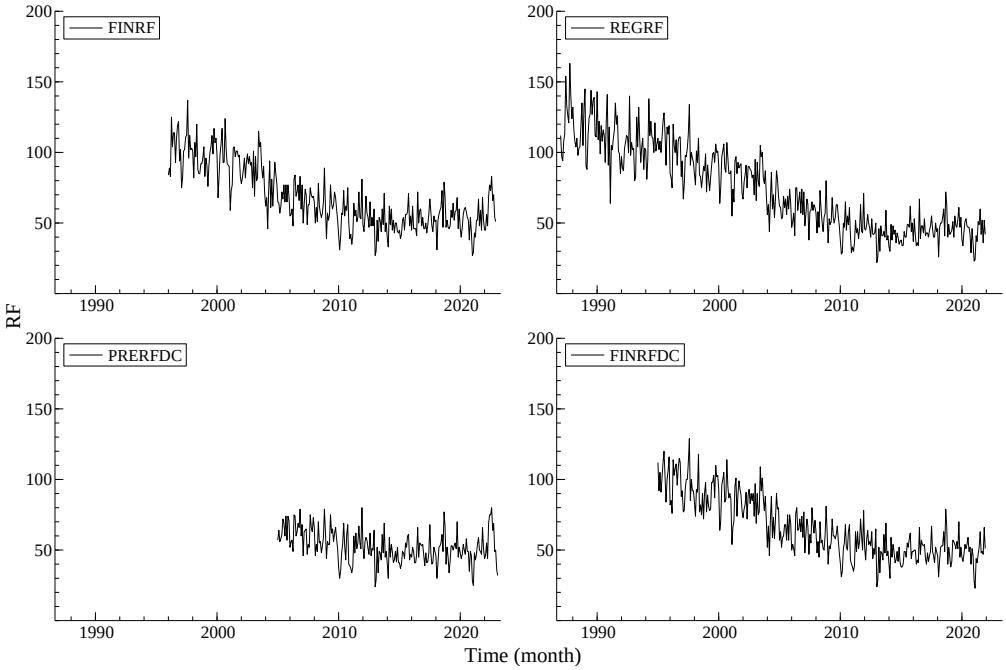


Figure SB1: Available monthly observations of the time series on the number of road fatalities.

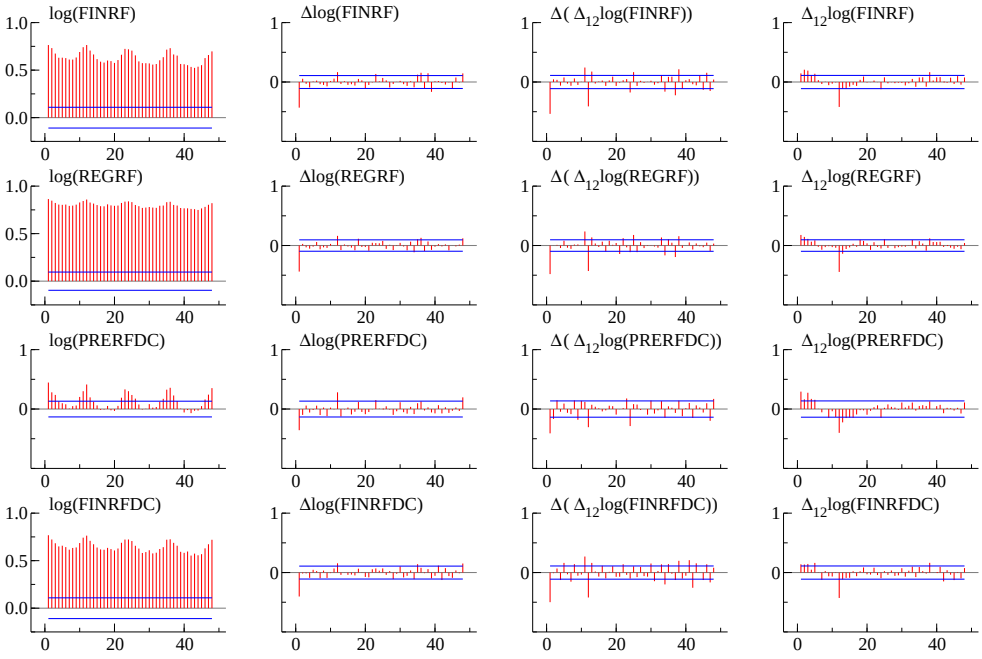


Figure SB2: Autocorrelation of road fatalities time series, in logs and after (seasonal) differencing.

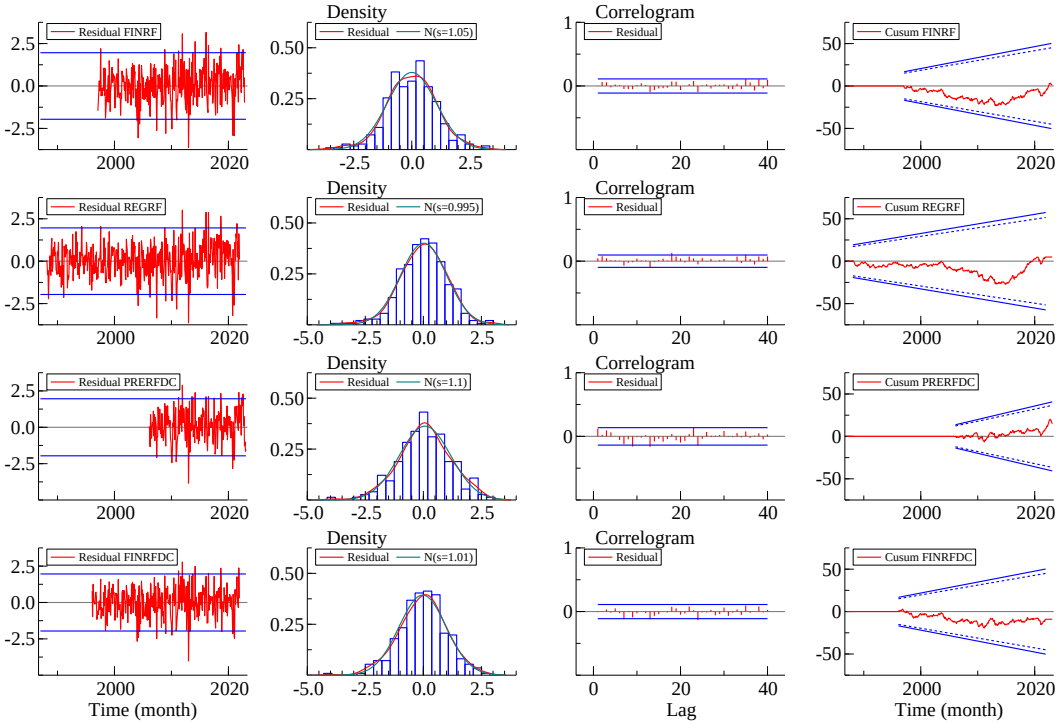


Figure SB3: Innovations diagnostics of Model 2, obtained with Kalman smoother.

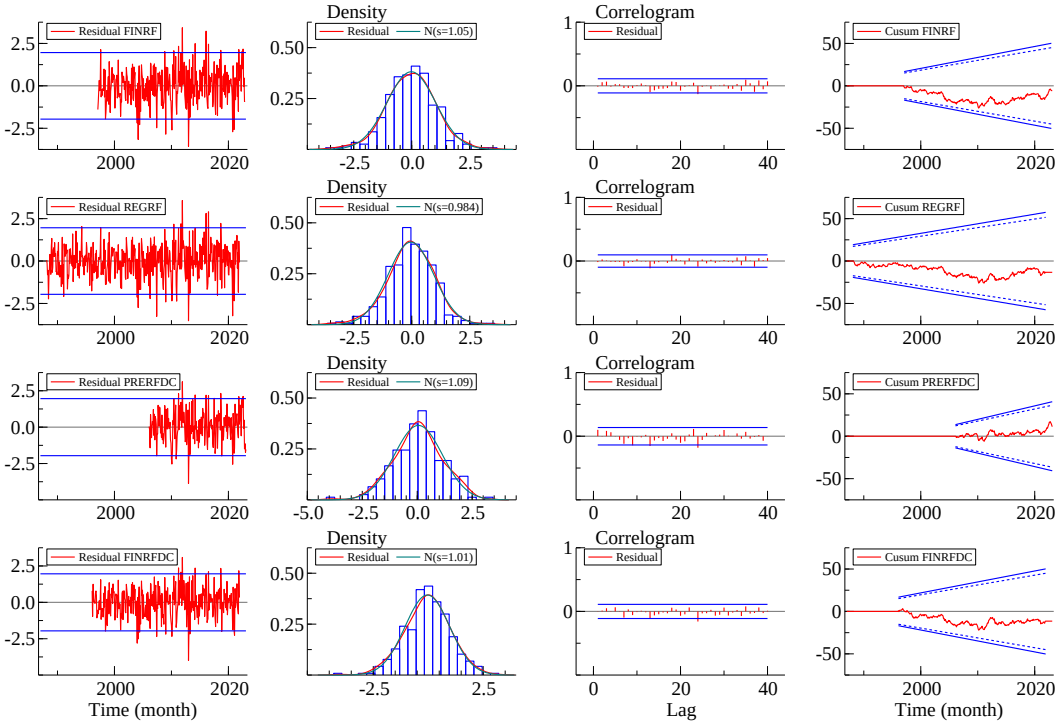


Figure SB4: Innovations diagnostics of Model 6, obtained with Kalman smoother.

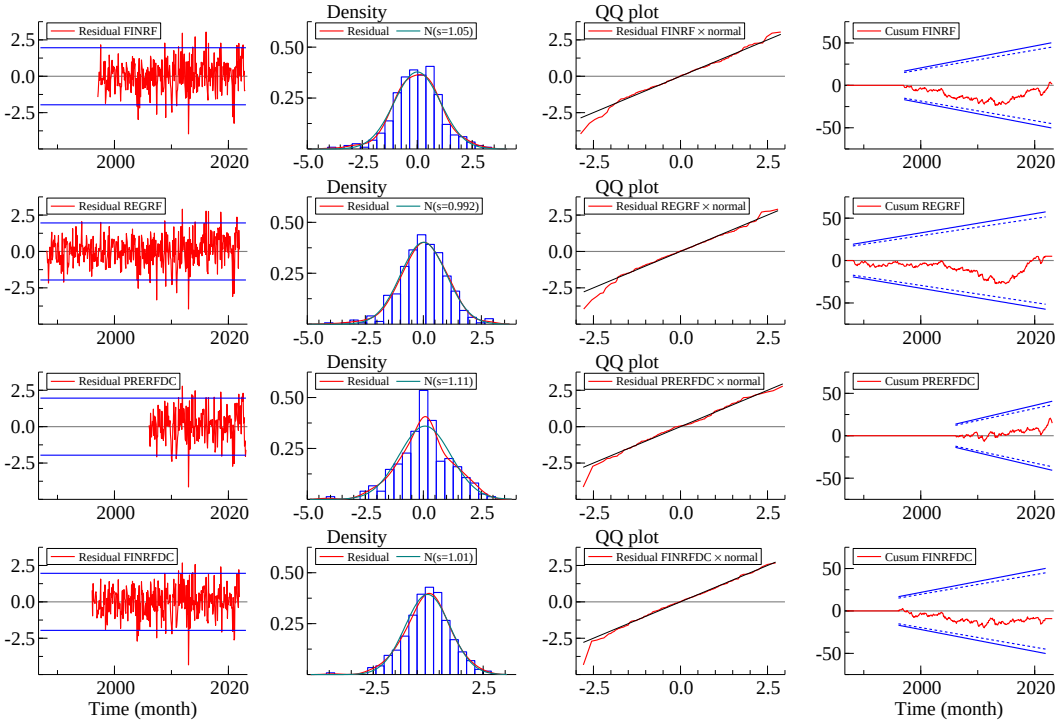


Figure SB5: Additional residual diagnostics of Model 1 including QQ plot.

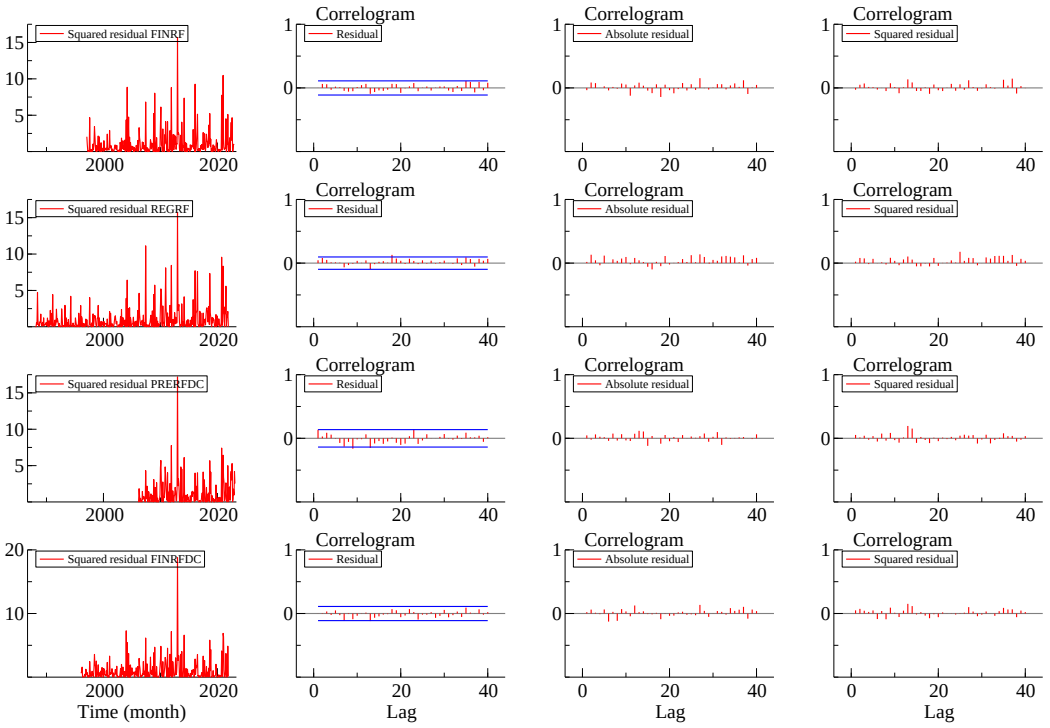


Figure SB6: Additional residual diagnostics of Model 1 including autocorrelation of absolute and squared residuals.

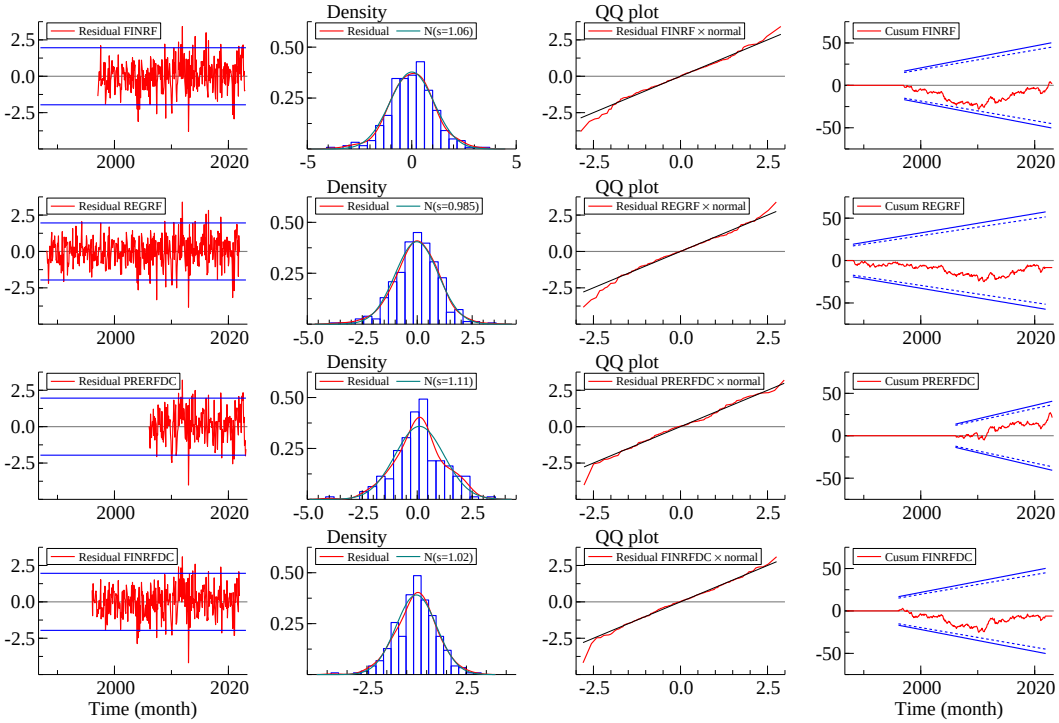


Figure SB7: Additional residual diagnostics of Model 4 including QQ plot.

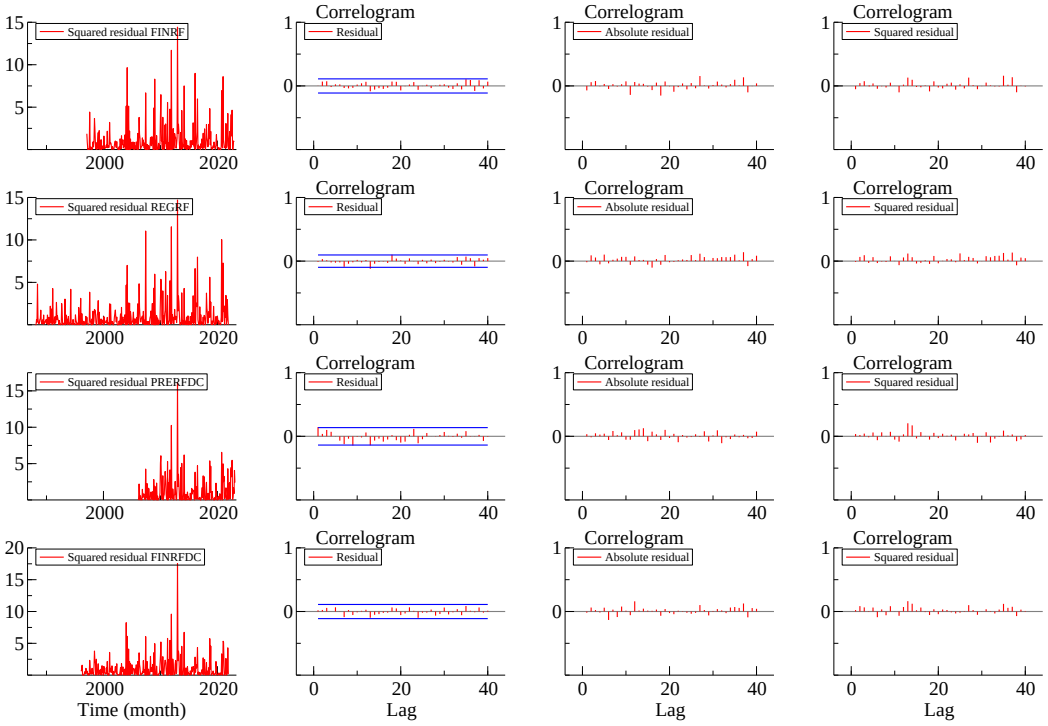


Figure SB8: Additional residual diagnostics of Model 4 including autocorrelation of absolute and squared residuals.

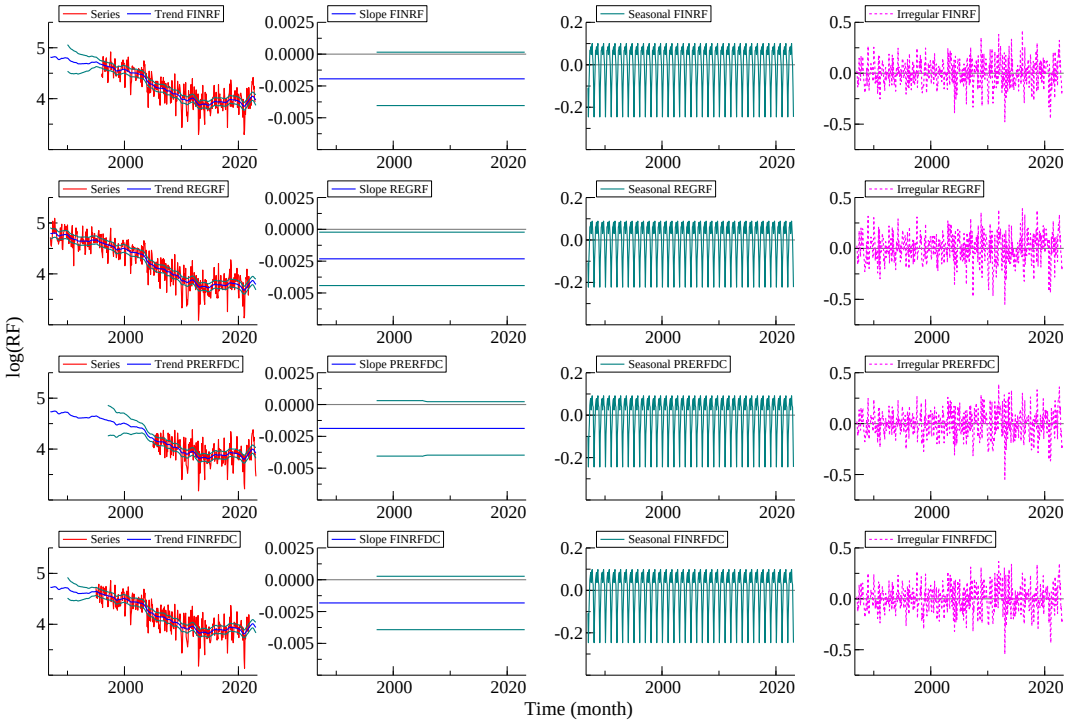


Figure SB9: State vector estimates in Model 1, obtained with Kalman smoother.

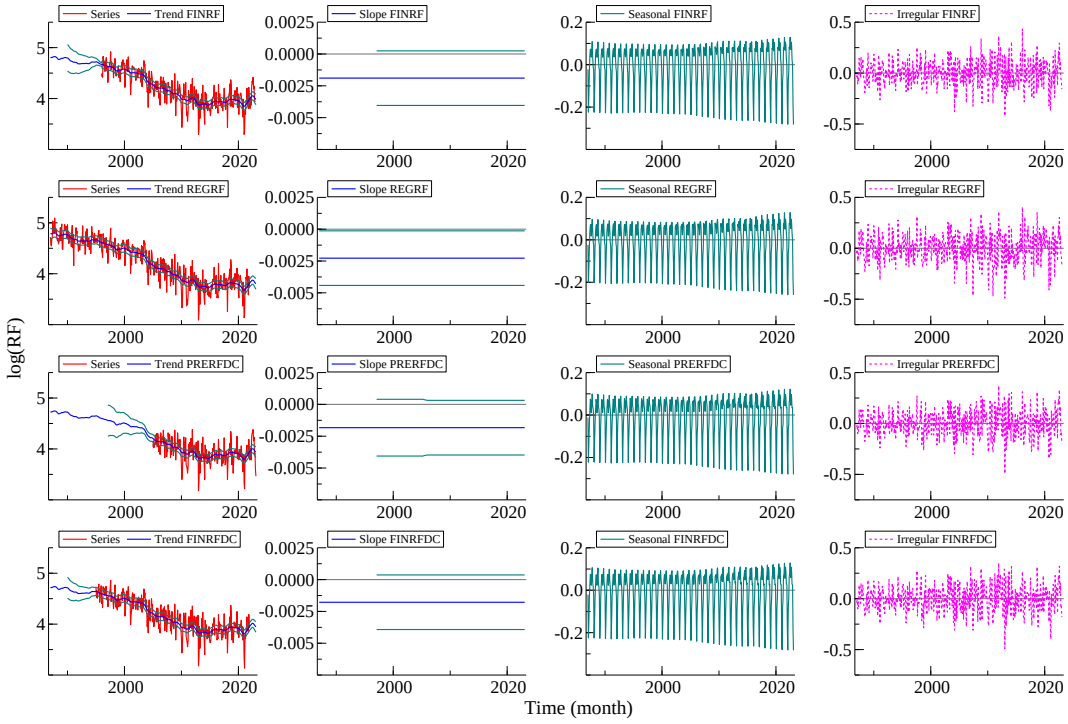


Figure SB10: State vector estimates in Model 2, obtained with Kalman smoother.

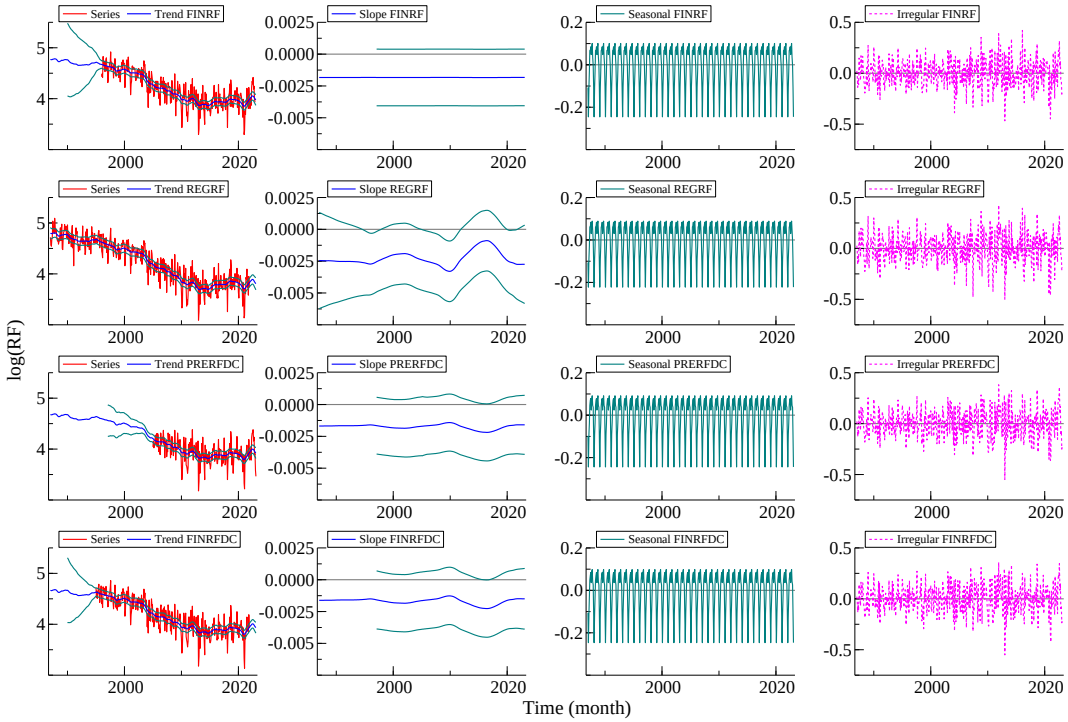


Figure SB11: State vector estimates in Model 3, obtained with Kalman smoother.

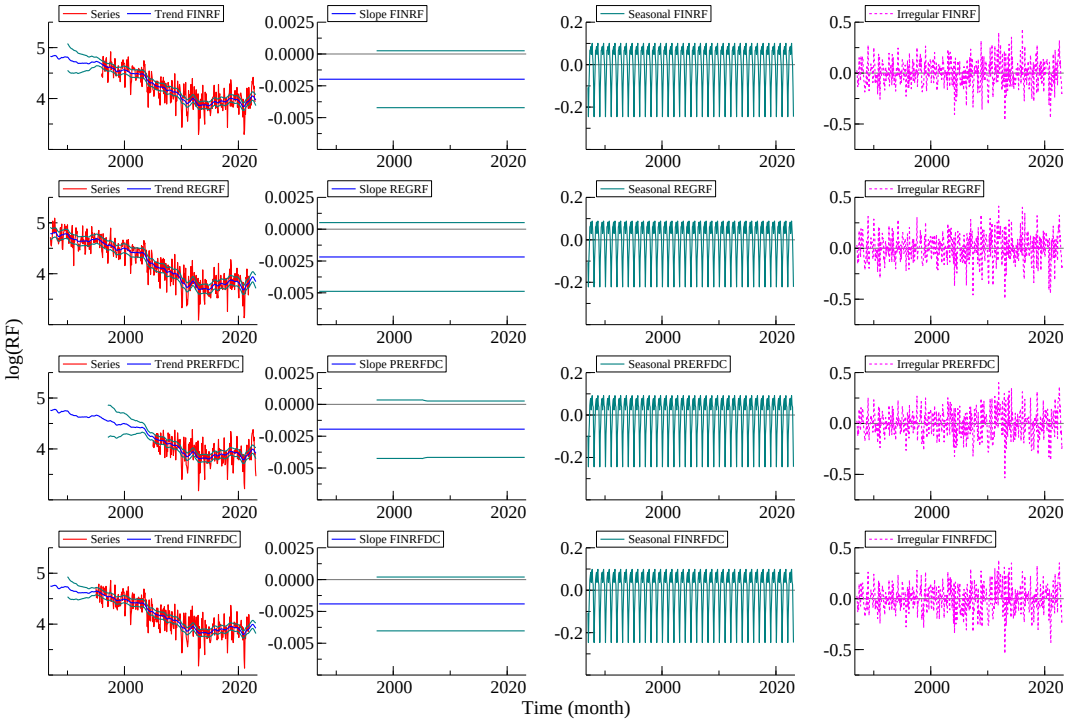


Figure SB12: State vector estimates in model 4, obtained with Kalman smoother.

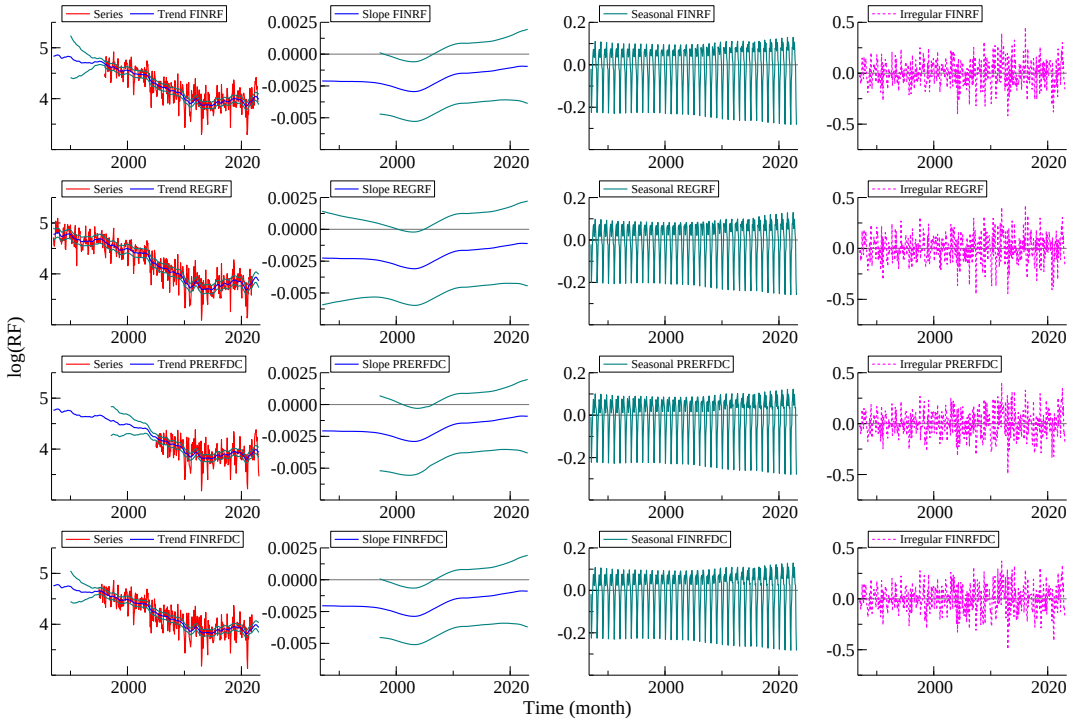


Figure SB13: State vector estimates in Model 5, obtained with Kalman smoother.

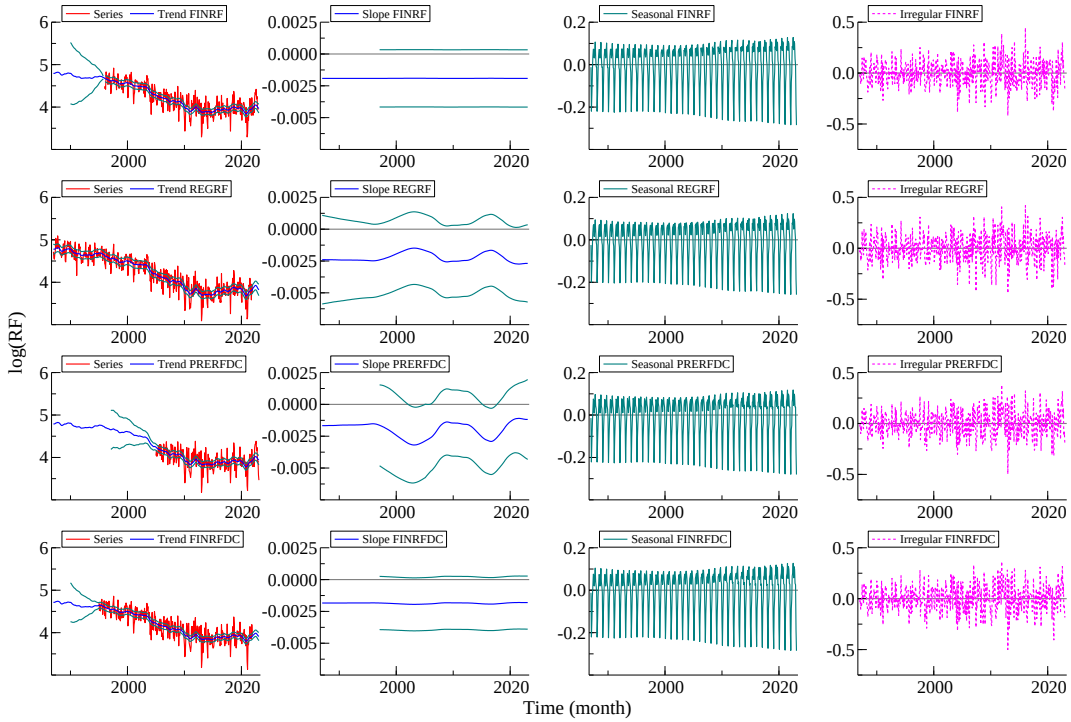


Figure SB14: State vector estimates in Model 6, obtained with Kalman smoother.

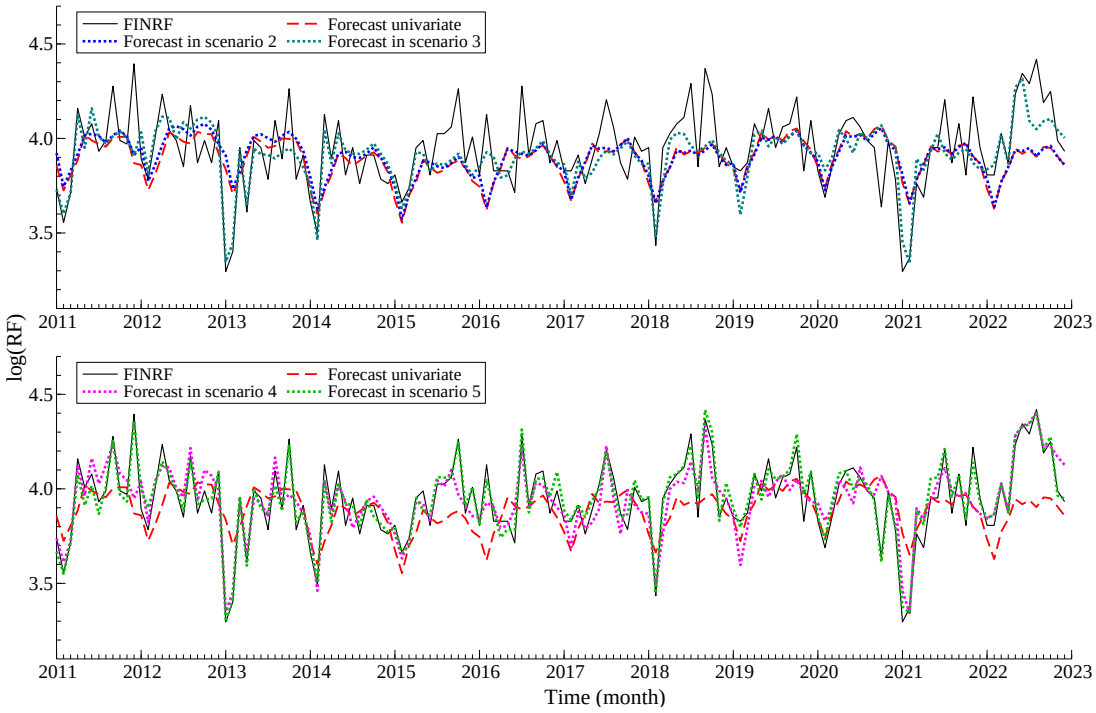


Figure SB15: 1- to 12-step ahead forecasts of the FINRF series of Model 1, in the different forecasting scenarios over the forecasting years 2011-2022.

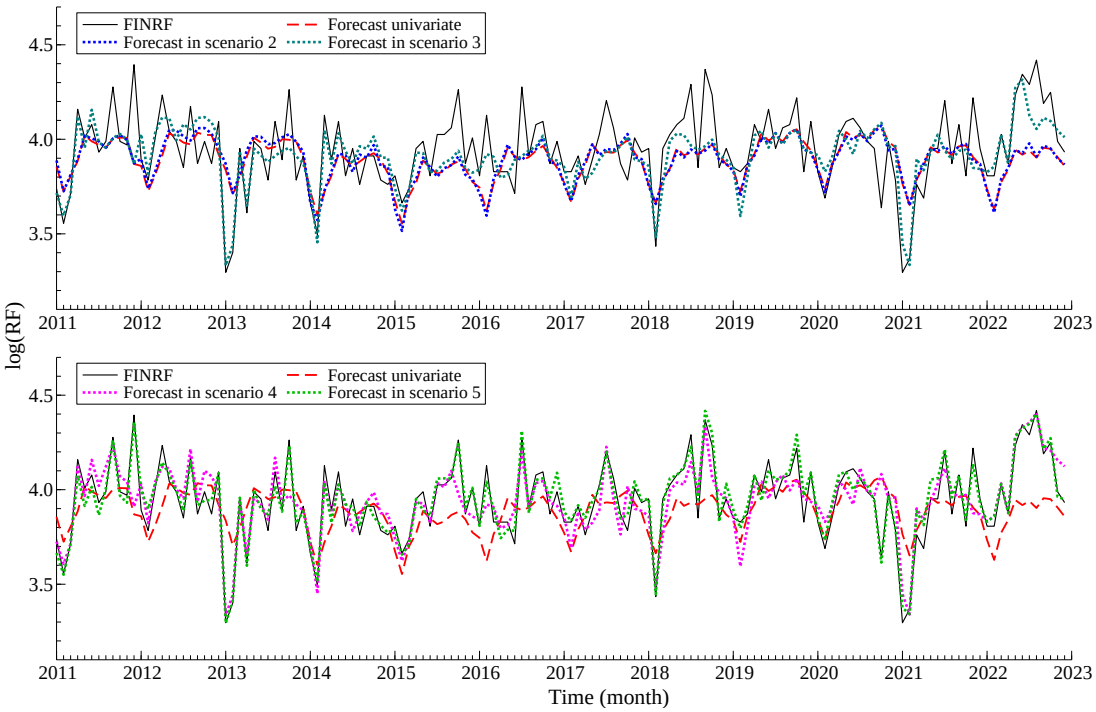


Figure SB16: 1- to 12-step ahead forecasts of the FINRF series of Model 2, in the different forecasting scenarios over the forecasting years 2011-2022.

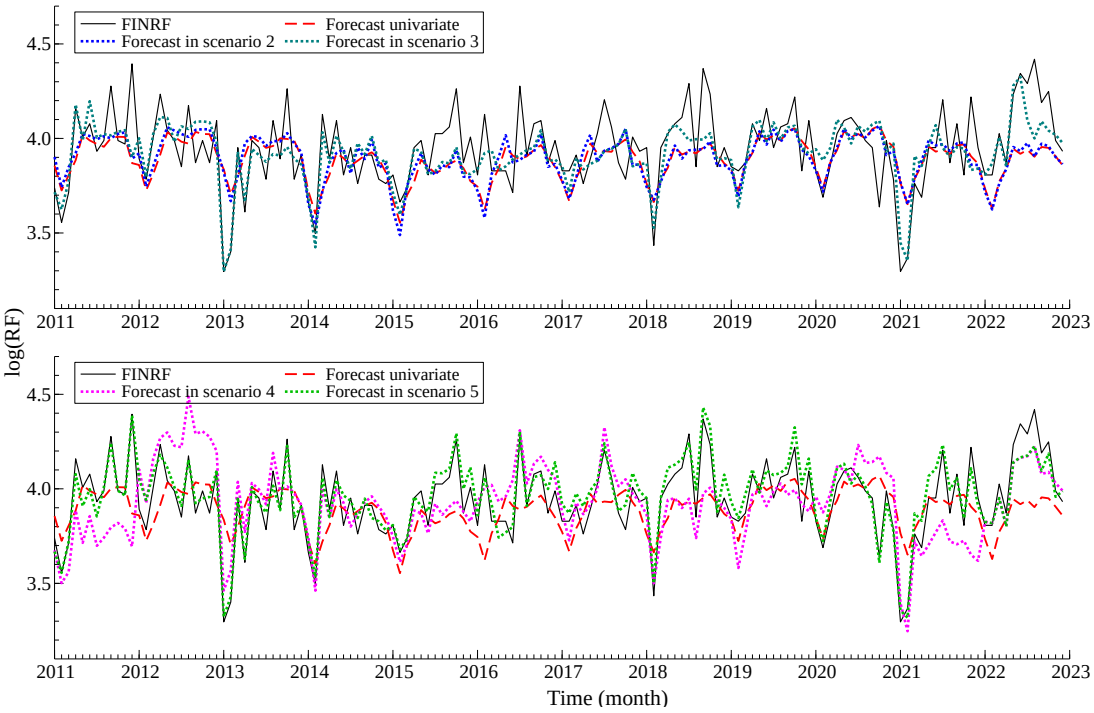


Figure SB17: 1- to 12-step ahead forecasts of the FINRF series of Model 3, in the different forecasting scenarios over the forecasting years 2011-2022.

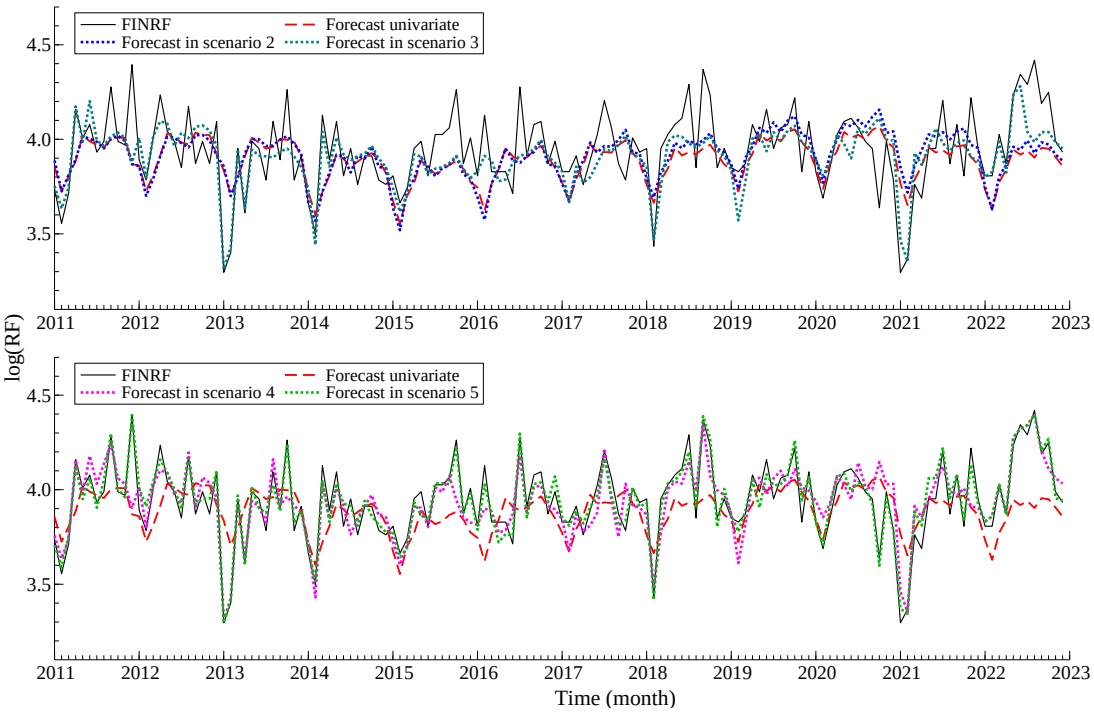


Figure SB18: 1- to 12-step ahead forecasts of the FINRF series of Model 5, in the different forecasting scenarios over the forecasting years 2011-2022.

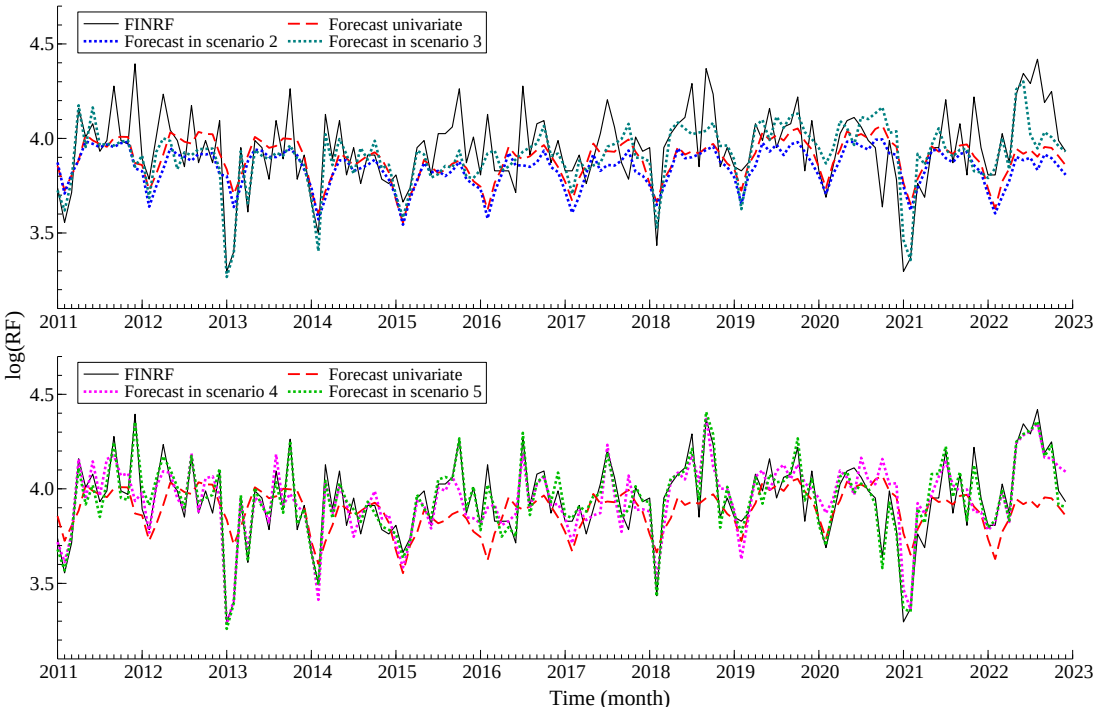


Figure SB19: 1- to 12-step ahead forecasts of the FINRF series of Model 6, in the different forecasting scenarios over the forecasting years 2011-2022.

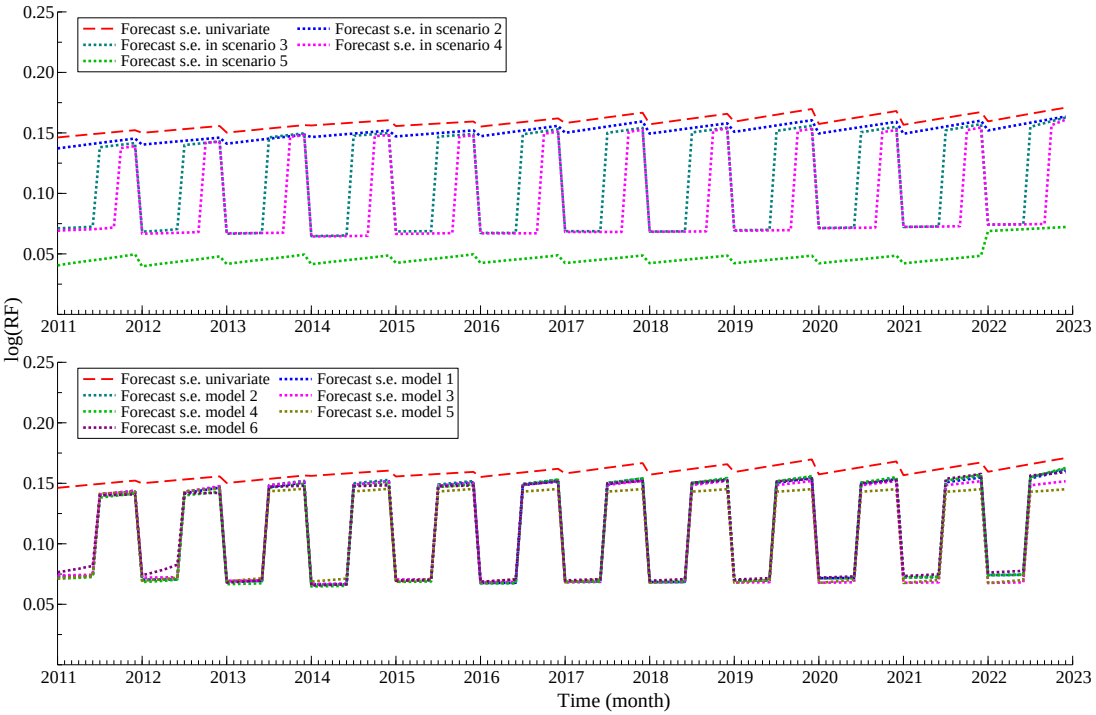


Figure SB20: 1- to 12-step ahead forecast standard errors comparison from model 4 in the different scenarios and of the different models in scenario 3 respectively.

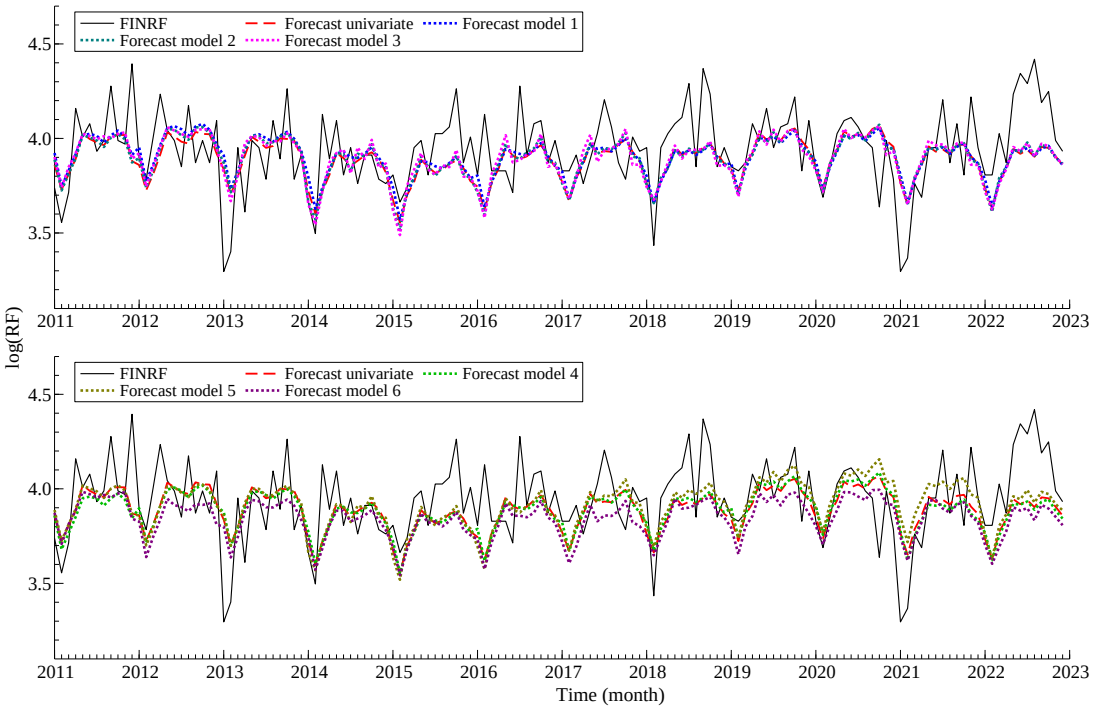


Figure SB21: 1- to 12-step ahead forecasts of the FINRF series of the different models in scenario 2, over the forecasting years 2011-2022.

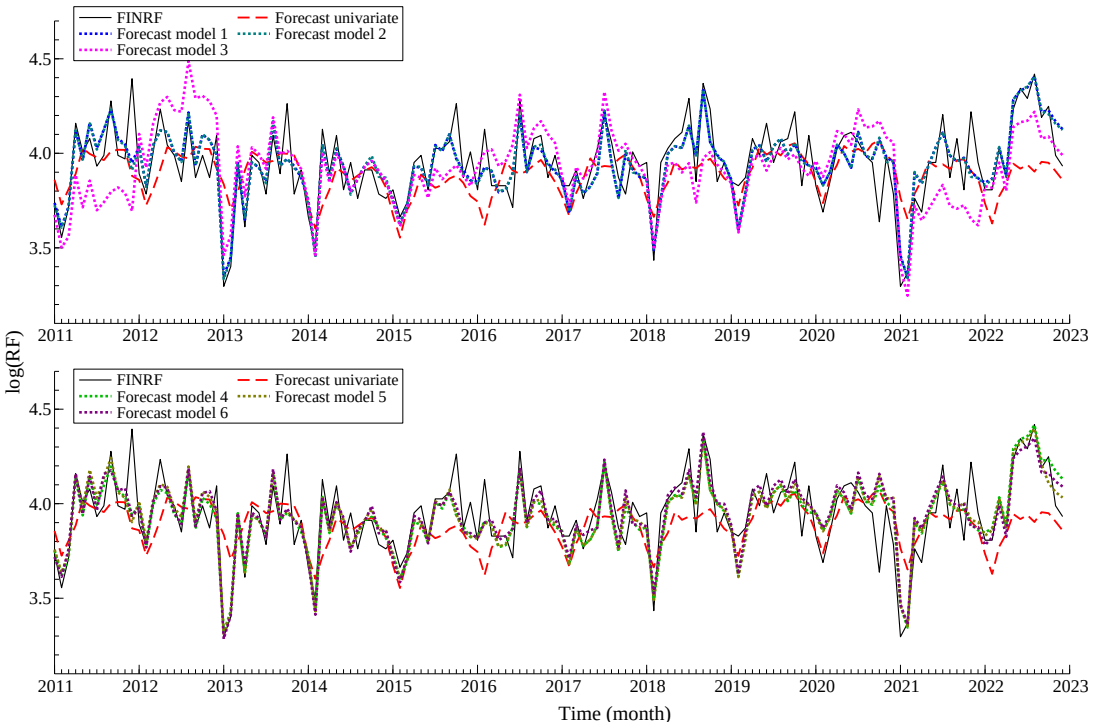


Figure SB22: 1- to 12-step ahead forecasts of the FINRF series of the different models in scenario 4, over the forecasting years 2011-2022.

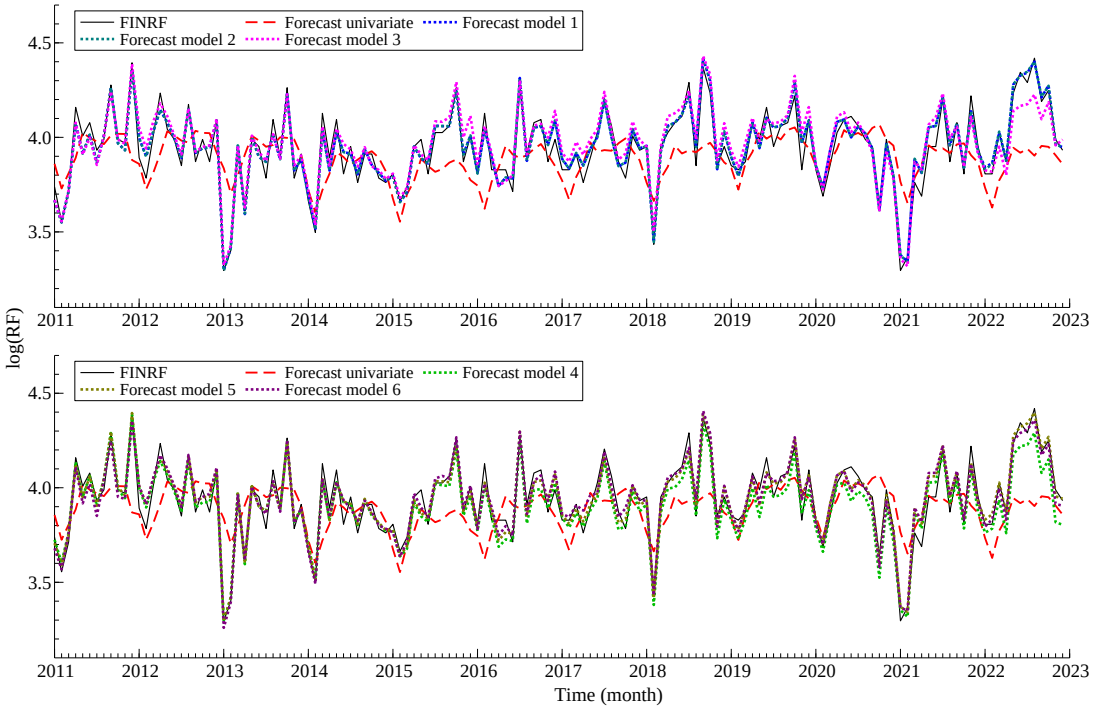


Figure SB23: 1- to 12-step ahead forecasts of the FINRF series of the different models in scenario 5, over the forecasting years 2011-2022.

# SC Supplementary material Section 4

## SC.1 Tables

Table SC1: Parameter estimates with constant (left) and time-varying (right) variances for trend disturbance terms.

| Model | 1 | 2 | 3 | 4 | 1 | 2 | 3 | 4 |
|---|---|---|---|---|---|---|---|---|
| $\hat{\sigma}^2_{\xi_1}$ | 0.1235 | 1.133e-08 | 0.0897 | 0.0914 | 0.0542 | 0.0519 | 0.0347 | 0.0342 |
| $\hat{\sigma}^2_{\xi_2}$ | - | - | 0.0475 | 0.0464 | - | - | 0.0324 | 0.0334 |
| $\hat{\theta}_{\mu_1,2}$ | 0.3278 | 1926.0761 | 0.4350 | 0.4371 | 0.3807 | 0.3993 | 0.4139 | 0.3704 |
| $\hat{\theta}_{\mu_1,3}$ | 0.3776 | 1784.4226 | 0.4788 | 0.4673 | 0.4218 | 0.4447 | 0.4717 | 0.4400 |
| $\hat{\theta}_{\mu_1,4}$ | 0.4553 | 1675.4192 | 0.3776 | 0.4069 | 0.4727 | 0.4859 | 0.5060 | 0.5275 |
| $\hat{\theta}_{\mu_2,3}$ | - | - | 0.7975 | 0.8017 | - | - | 0.7224 | 0.7313 |
| $\hat{\theta}_{\mu_2,4}$ | - | - | -0.0140 | -0.0359 | - | - | -0.1390 | -0.1174 |
| $\hat{\sigma}^2_{\zeta_1}$ | 0.0072 | 0.0340 | 0.0179 | 0.0176 | 0.0052 | 0.0050 | 0.0087 | 0.0089 |
| $\hat{\sigma}^2_{\zeta_2}$ | - | - | 0.0007 | 0.0007 | - | - | 0.0007 | 0.0007 |
| $\hat{\theta}_{\nu_1,2}$ | 1.1395 | 0.5876 | 0.6442 | 0.6461 | 1.1454 | 1.1593 | 0.7712 | 0.7627 |
| $\hat{\theta}_{\nu_1,3}$ | 1.1814 | 0.6770 | 0.7726 | 0.7715 | 1.1845 | 1.1975 | 0.8793 | 0.8661 |
| $\hat{\theta}_{\nu_1,4}$ | 1.2859 | 0.7931 | 0.9999 | 0.9925 | 1.2848 | 1.2962 | 1.0588 | 1.0407 |
| $\hat{\theta}_{\nu_2,3}$ | - | - | 0.9542 | 0.9548 | - | - | 0.9882 | 0.9887 |
| $\hat{\theta}_{\nu_2,4}$ | - | - | 1.0569 | 1.0719 | - | - | 1.1712 | 1.1911 |
| $\hat{\sigma}^2_{\omega_1}$ | 0.0029 | 0 | 0.0039 | 0.0041 | 0.0043 | 1.924e-08 | 0.0058 | 0.0049 |
| $\hat{\sigma}^2_{\omega_2}$ | - | 0 | - | 3.393e-11 | - | 5.117e-10 | - | 1.818e-11 |
| $\hat{\sigma}^2_{\omega_3}$ | - | 0 | - | 0.0002 | - | 0.0011 | - | 0.0006 |
| $\hat{\sigma}^2_{\omega_4}$ | - | 0 | - | 4.369e-13 | - | 6.545e-10 | - | 7.151e-12 |
| $\hat{\theta}_{\gamma_1,2}$ | 0.0086 | - | 0.0909 | - | -0.2016 | - | -0.0983 | - |
| $\hat{\theta}_{\gamma_1,3}$ | -0.4189 | - | -0.2201 | - | -0.6199 | - | -0.4127 | - |
| $\hat{\theta}_{\gamma_1,4}$ | 0.0714 | - | 0.0483 | - | -0.0281 | - | -0.0517 | - |
| $\hat{\sigma}^2_{e}$ | 1.1865 | 0.9902 | 0.4702 | 0.4652 | 1.1567 | 1.1661 | 0.5213 | 0.5280 |
| $\hat{\sigma}^2_{\varepsilon_y}$ | 2.933e-18 | 0.0535 | 4.697e-08 | 1.015e-19 | 3.173e-12 | 0.0268 | 3.213e-09 | 0.0029 |
| $\hat{\sigma}^2_{\varepsilon_x}$ | 1.243e-07 | 0.0049 | 0.0151 | 0.0155 | 5.255e-10 | 2.253e-05 | 0.0134 | 0.0129 |

Table SC2: Ljung-Box test statistics for different lag sizes. Test statistic is asymptotically chi-square distributed with df: lag size - (# parameters/$N$) - 1.

| | | | | constant trend variance | | | | time-varying trend variance | | | |
|---|---|---|---|---|---|---|---|---|---|---|---|
| Model | | | | 1 | 2 | 3 | 4 | 1 | 2 | 3 | 4 |
| Series | lag size | lowest df | crit. value | | | | | | | | |
| $y_t$ | 20 | 14 | 23.685 | 9.429 | 21.158 | 9.392 | 9.372 | 15.910 | 35.065** | 10.482 | 10.991 |
| | 30 | 24 | 36.415 | 11.678 | 26.849 | 13.710 | 14.374 | 18.788 | 46.087** | 15.730 | 17.686 |
| | 40 | 34 | 48.602 | 16.259 | 35.787 | 22.546 | 23.265 | 21.572 | 56.679** | 22.256 | 24.979 |
| | 50 | 44 | 60.481 | 32.293 | 54.417 | 38.613 | 38.723 | 37.997 | 76.769** | 36.627 | 40.294 |
| | 60 | 54 | 72.153 | 50.925 | 63.059 | 47.504 | 47.512 | 61.435 | 93.235** | 49.724 | 52.905 |
| $x_{t,1}$ | 20 | 14 | 23.685 | 18.935 | 17.592 | 20.862 | 20.202 | 24.466* | 23.942* | 30.117** | 29.522** |
| | 30 | 24 | 36.415 | 33.372 | 30.302 | 36.544* | 36.290* | 43.444** | 41.790* | 52.419** | 50.221** |
| | 40 | 34 | 48.602 | 40.963 | 39.016 | 44.656 | 43.299 | 48.517 | 49.737* | 58.451** | 58.203** |
| | 50 | 44 | 60.481 | 63.366* | 63.535* | 64.573* | 63.251* | 68.646* | 68.841** | 71.478** | 70.888** |
| | 60 | 54 | 72.153 | 72.142 | 71.201 | 73.533* | 72.057 | 76.437* | 76.905* | 79.728* | 78.904* |
| $x_{t,2}$ | 20 | 14 | 23.685 | 12.577 | 10.971 | 11.201 | 11.402 | 16.883 | 12.892 | 15.186 | 11.295 |
| | 30 | 24 | 36.415 | 21.490 | 15.911 | 20.245 | 20.478 | 27.503 | 21.541 | 23.990 | 19.973 |
| | 40 | 34 | 48.602 | 24.604 | 19.825 | 23.514 | 24.916 | 32.395 | 26.884 | 27.913 | 27.166 |
| | 50 | 44 | 60.481 | 36.324 | 30.960 | 35.336 | 36.935 | 47.072 | 37.640 | 41.128 | 36.974 |
| | 60 | 54 | 72.153 | 53.921 | 47.549 | 52.598 | 52.823 | 65.384 | 52.317 | 60.302 | 50.637 |
| $x_{t,3}$ | 20 | 14 | 23.685 | 60.199** | 30.718** | 32.893** | 32.484** | 64.063** | 64.517** | 35.344** | 35.134** |
| | 30 | 24 | 36.415 | 76.011** | 38.536* | 44.108** | 43.599** | 81.061** | 81.161** | 47.819** | 47.355** |
| | 40 | 34 | 48.602 | 86.697** | 46.628 | 48.675* | 48.289 | 92.242** | 92.372** | 56.138** | 55.635** |
| | 50 | 44 | 60.481 | 106.486** | 56.814 | 62.458* | 62.202* | 112.190** | 112.902** | 72.647** | 72.635** |
| | 60 | 54 | 72.153 | 120.576** | 63.274 | 71.013 | 70.788 | 125.529** | 126.574** | 83.857** | 83.608** |
| # parameters | | | | 15 | 15 | 21 | 21 | 15 | 15 | 21 | 21 |

$^{**}p < 0.01$, $^{*}p < 0.05$

Table SC3: MAPE forecasting performance based on the 5-step ahead forecasts per forecasting year and in total relative to the MAPE of the univariate benchmark model (BSTS), for models with time constant (Const.) and time-varying (TV) variances for trend disturbance terms.

| Scenario | Model | 2011 | 2012 | 2013 | 2014 | 2015 | 2016 | 2017 | 2018 | 2019 | 2020 | | 2021 | | Total | |
|---|---|---|---|---|---|---|---|---|---|---|---|---|---|---|---|---|
| | | | | | | | | | | | Const. | TV | Const. | TV | Const. | TV |
| 1 | BSTS | 1.000 | 1.000 | 1.000 | 1.000 | 1.000 | 1.000 | 1.000 | 1.000 | 1.000 | 1.000 | 1.000 | 1.000 | 1.000 | 1.000 | 1.000 |
| 2 | 1 | 1.092 | 0.599 | 0.578 | 1.763 | 0.747 | 1.441 | 0.981 | 0.713 | 1.263 | 0.643 | 1.013 | 0.331 | 0.778 | 0.695 | 0.903 |
| | 2 | 0.933 | 0.485 | 0.672 | 1.535 | 0.679 | 1.402 | 0.910 | 0.533 | 1.019 | 0.624 | 1.060 | 0.340 | 0.831 | 0.639 | 0.877 |
| | 3 | 0.660 | 0.540 | 0.407 | 1.696 | 0.742 | 1.651 | 1.244 | 1.028 | 1.580 | 0.626 | 1.045 | 0.309 | 0.380 | 0.640 | 0.727 |
| | 4 | 0.830 | 0.626 | 0.914 | 1.989 | 0.319 | 1.421 | 2.363 | 0.715 | 0.820 | 0.511 | 0.586 | 0.334 | 0.611 | 0.644 | 0.788 |
| 3 | 1 | 1.089 | 0.599 | 0.615 | 1.658 | 0.770 | 1.558 | 1.147 | 1.056 | 1.100 | 0.618 | 0.978 | 0.350 | 0.817 | 0.705 | 0.919 |
| | 2 | 0.955 | 0.486 | 0.649 | 1.433 | 0.698 | 1.513 | 1.143 | 0.868 | 0.864 | 0.606 | 1.009 | 0.352 | 0.867 | 0.651 | 0.892 |
| | 3 | 0.540 | 0.850 | 0.881 | 2.221 | 0.500 | 0.878 | 3.321 | 1.564 | 0.649 | 0.509 | 0.589 | 0.347 | 0.260 | 0.675 | 0.638 |
| | 4 | 0.838 | 1.008 | 1.289 | 2.142 | 0.302 | 0.762 | 2.874 | 1.348 | 0.660 | 0.492 | 0.557 | 0.358 | 0.634 | 0.709 | 0.802 |
| 4 | 1 | 1.069 | 0.482 | 0.238 | 1.090 | 0.679 | 1.403 | 1.501 | 1.446 | 1.360 | 0.586 | 0.807 | 0.348 | 0.735 | 0.654 | 0.838 |
| | 2 | 0.840 | 0.484 | 0.732 | 1.695 | 0.626 | 1.398 | 0.814 | 0.767 | 0.980 | 0.572 | 0.899 | 0.342 | 0.860 | 0.625 | 0.854 |
| | 3 | 0.677 | 0.604 | 0.660 | 1.798 | 0.398 | 1.056 | 2.852 | 1.547 | 1.438 | 0.511 | 0.502 | 0.338 | 0.596 | 0.643 | 0.691 |
| | 4 | 0.816 | 0.585 | 0.870 | 1.932 | 0.331 | 0.818 | 2.256 | 2.382 | 1.089 | 0.503 | 0.491 | 0.348 | 0.286 | 0.661 | 0.665 |

Table SC4: MAE forecasting performance based on the 5-step ahead forecasts per forecasting year and in total relative to the MAE of the univariate benchmark model (BSTS), for models with time constant (Const.) and time-varying (TV) variances for trend disturbance terms.

| Scenario | Model | 2011 | 2012 | 2013 | 2014 | 2015 | 2016 | 2017 | 2018 | 2019 | 2020 | | 2021 | | Total | |
|---|---|---|---|---|---|---|---|---|---|---|---|---|---|---|---|---|
| | | | | | | | | | | | Const. | TV | Const. | TV | Const. | TV |
| 1 | BSTS | 1.000 | 1.000 | 1.000 | 1.000 | 1.000 | 1.000 | 1.000 | 1.000 | 1.000 | 1.000 | 1.000 | 1.000 | 1.000 | 1.000 | 1.000 |
| 2 | 1 | 1.089 | 0.597 | 0.578 | 1.760 | 0.747 | 1.444 | 0.979 | 0.715 | 1.261 | 0.644 | 1.014 | 0.327 | 0.776 | 0.688 | 0.901 |
| | 2 | 0.932 | 0.484 | 0.672 | 1.533 | 0.679 | 1.405 | 0.909 | 0.534 | 1.017 | 0.625 | 1.060 | 0.335 | 0.829 | 0.633 | 0.877 |
| | 3 | 0.659 | 0.538 | 0.406 | 1.692 | 0.741 | 1.655 | 1.242 | 1.030 | 1.577 | 0.627 | 1.045 | 0.305 | 0.374 | 0.636 | 0.722 |
| | 4 | 0.829 | 0.624 | 0.914 | 1.985 | 0.319 | 1.424 | 2.366 | 0.715 | 0.819 | 0.512 | 0.586 | 0.331 | 0.610 | 0.638 | 0.783 |
| 3 | 1 | 1.087 | 0.598 | 0.615 | 1.655 | 0.769 | 1.562 | 1.146 | 1.058 | 1.099 | 0.619 | 0.978 | 0.345 | 0.814 | 0.699 | 0.917 |
| | 2 | 0.954 | 0.485 | 0.649 | 1.431 | 0.698 | 1.517 | 1.142 | 0.871 | 0.863 | 0.607 | 1.009 | 0.348 | 0.864 | 0.645 | 0.891 |
| | 3 | 0.539 | 0.849 | 0.881 | 2.217 | 0.498 | 0.881 | 3.329 | 1.568 | 0.648 | 0.509 | 0.589 | 0.343 | 0.257 | 0.669 | 0.631 |
| | 4 | 0.837 | 1.007 | 1.289 | 2.138 | 0.302 | 0.765 | 2.881 | 1.350 | 0.660 | 0.492 | 0.557 | 0.355 | 0.633 | 0.701 | 0.797 |
| 4 | 1 | 1.067 | 0.482 | 0.238 | 1.089 | 0.679 | 1.405 | 1.501 | 1.448 | 1.361 | 0.585 | 0.807 | 0.344 | 0.734 | 0.650 | 0.838 |
| | 2 | 0.839 | 0.483 | 0.732 | 1.693 | 0.626 | 1.400 | 0.814 | 0.769 | 0.980 | 0.572 | 0.898 | 0.337 | 0.858 | 0.619 | 0.853 |
| | 3 | 0.676 | 0.603 | 0.659 | 1.793 | 0.398 | 1.056 | 2.851 | 1.551 | 1.436 | 0.511 | 0.501 | 0.333 | 0.594 | 0.639 | 0.690 |
| | 4 | 0.815 | 0.583 | 0.870 | 1.927 | 0.330 | 0.818 | 2.264 | 2.383 | 1.087 | 0.503 | 0.491 | 0.344 | 0.282 | 0.656 | 0.658 |

## SC.2 Figures

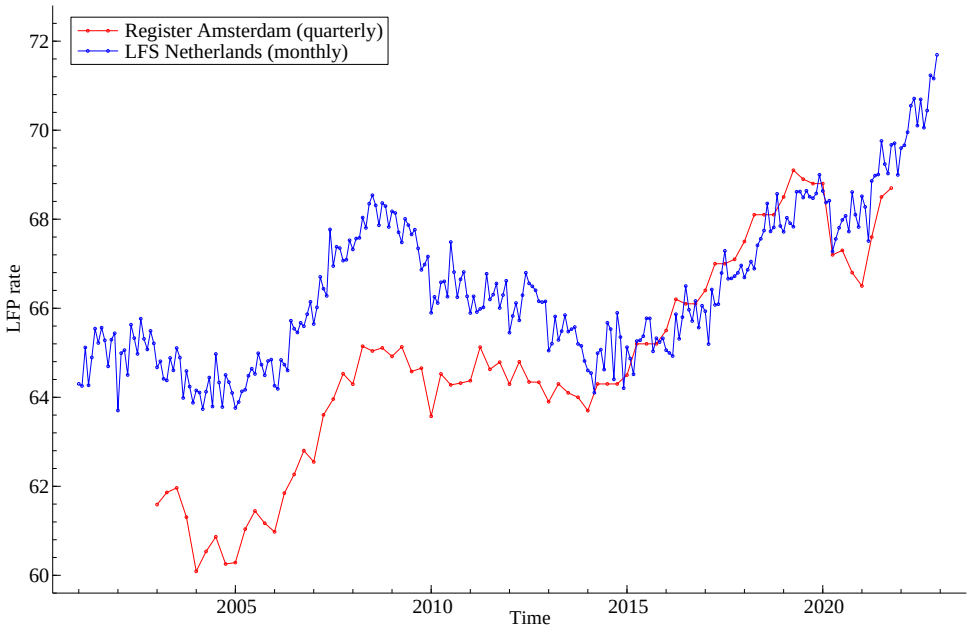


Figure SC1: Available time series of quarterly labour force participation (LFP) rate in Amsterdam derived from the tax register and monthly LFP rate in the Netherlands obtained from the labour force survey.

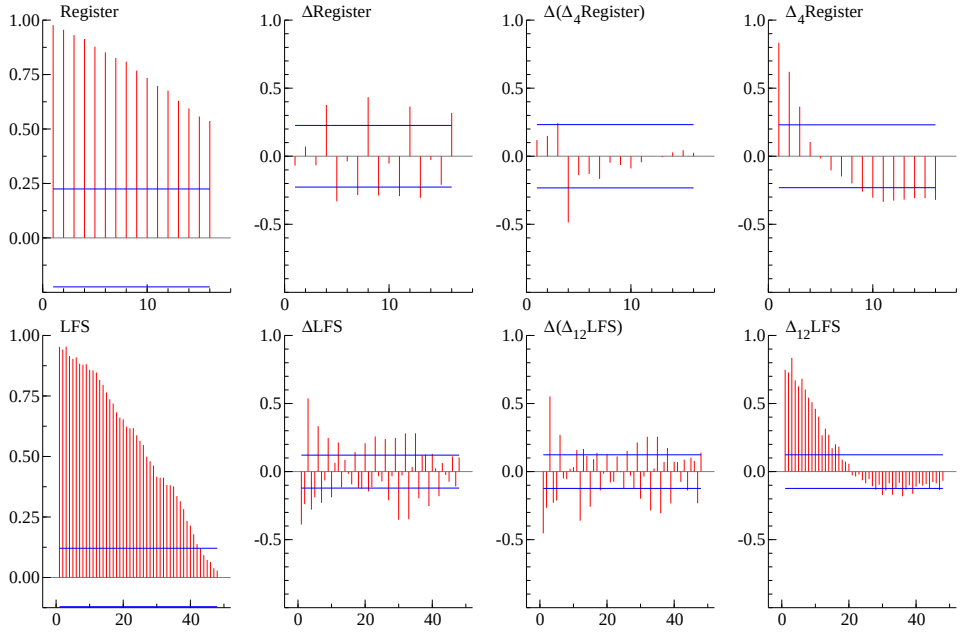


Figure SC2: Autocorrelation of labour force time series, in levels and after (seasonal) differencing.

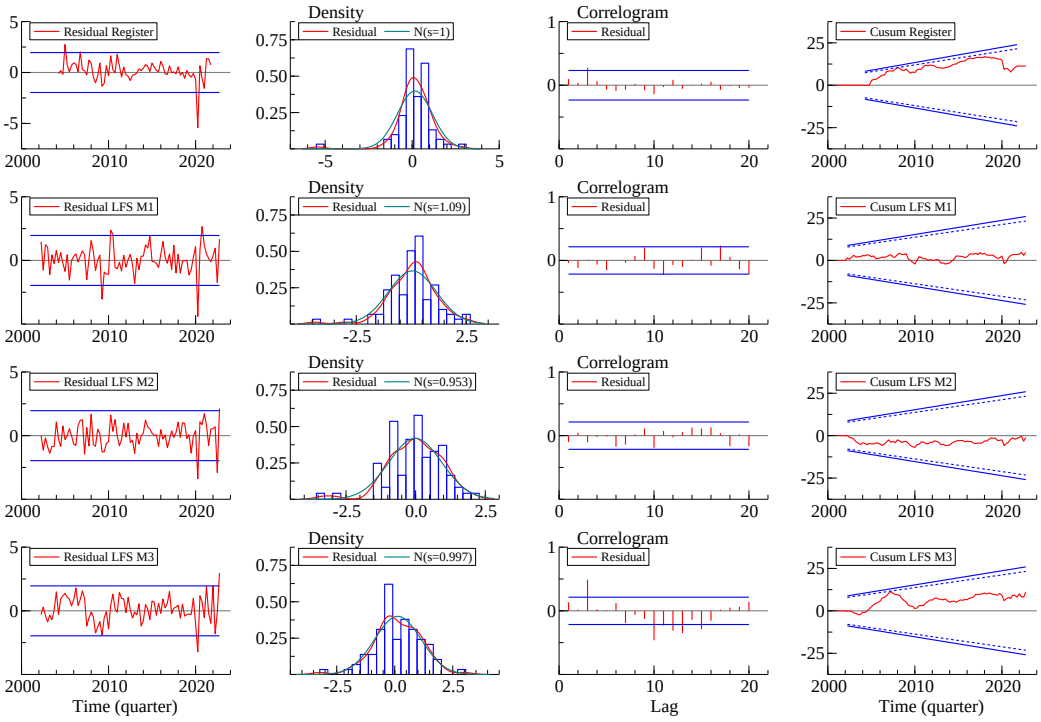


Figure SC3: Innovations diagnostics of Model 1, obtained with Kalman smoother.

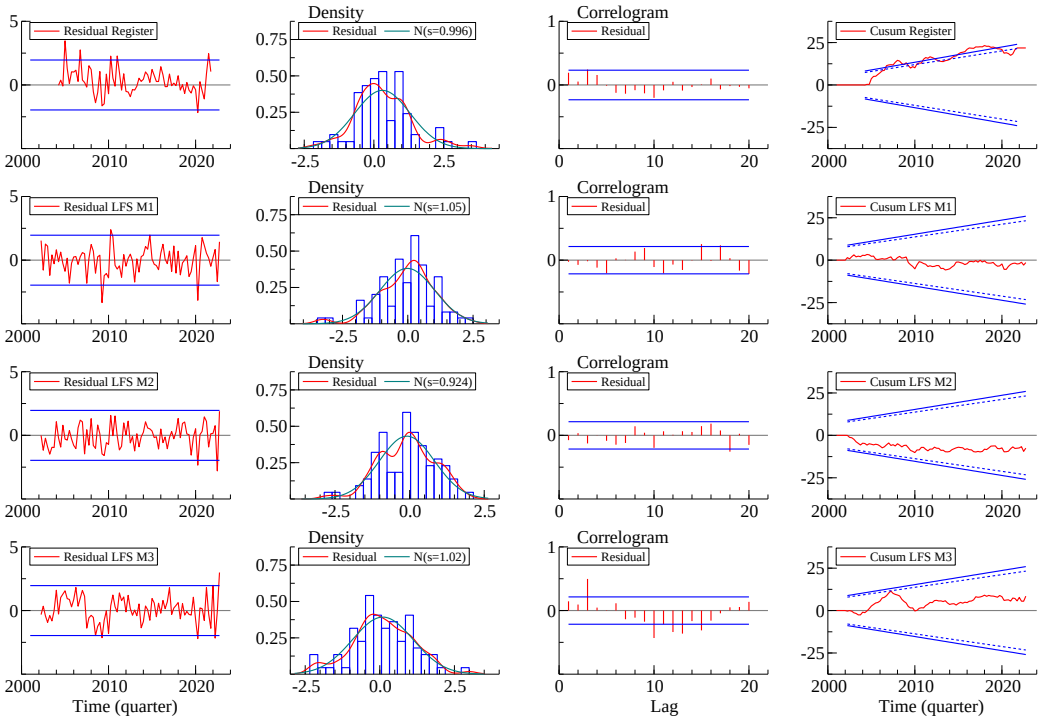


Figure SC4: Innovations diagnostics of Model 1 including time-varying variances for the trend disturbance terms at the start of the COVID-19 outbreak.

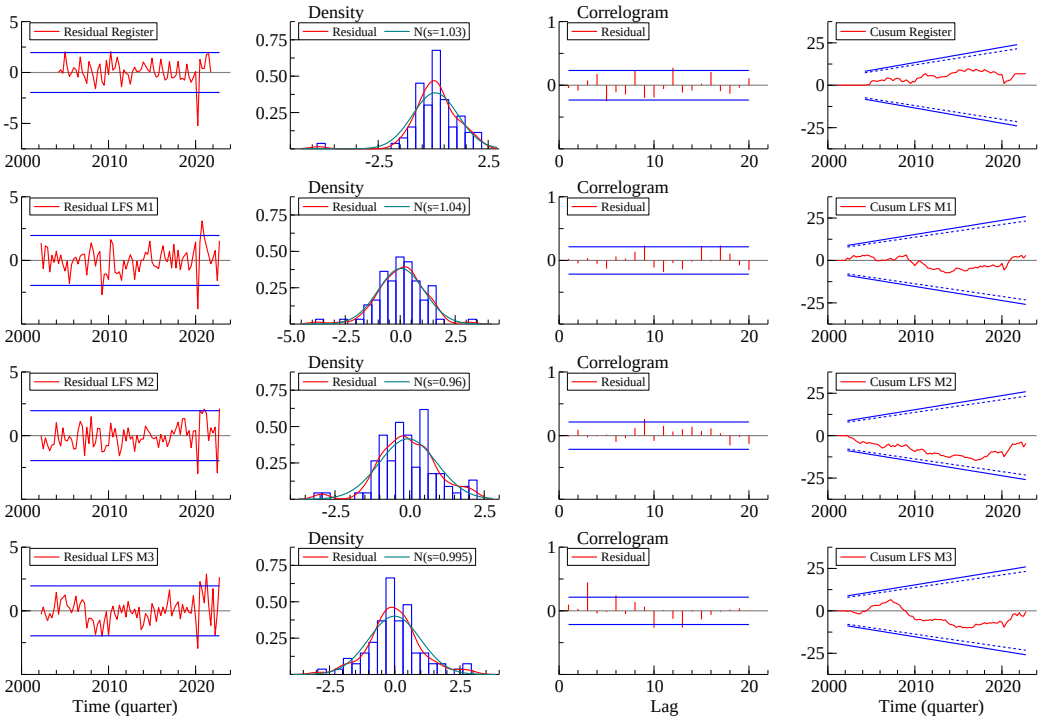


Figure SC5: Innovations diagnostics of Model 2, obtained with Kalman smoother.

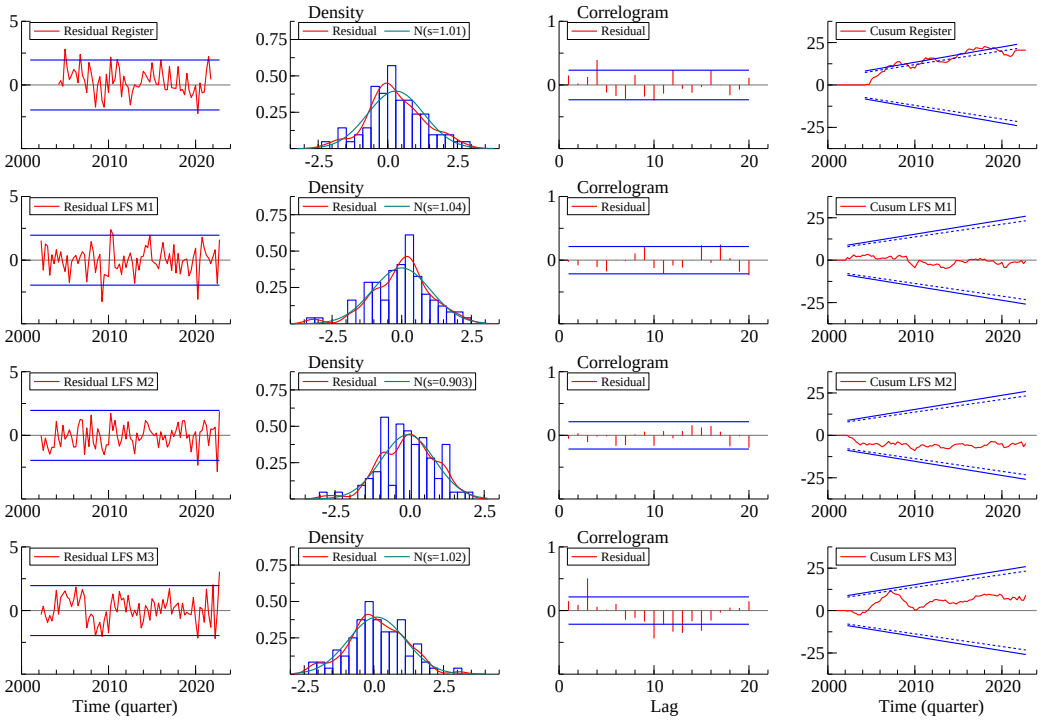


Figure SC6: Innovations diagnostics of Model 2 including time-varying variances for the trend disturbance terms at the start of the COVID-19 outbreak.

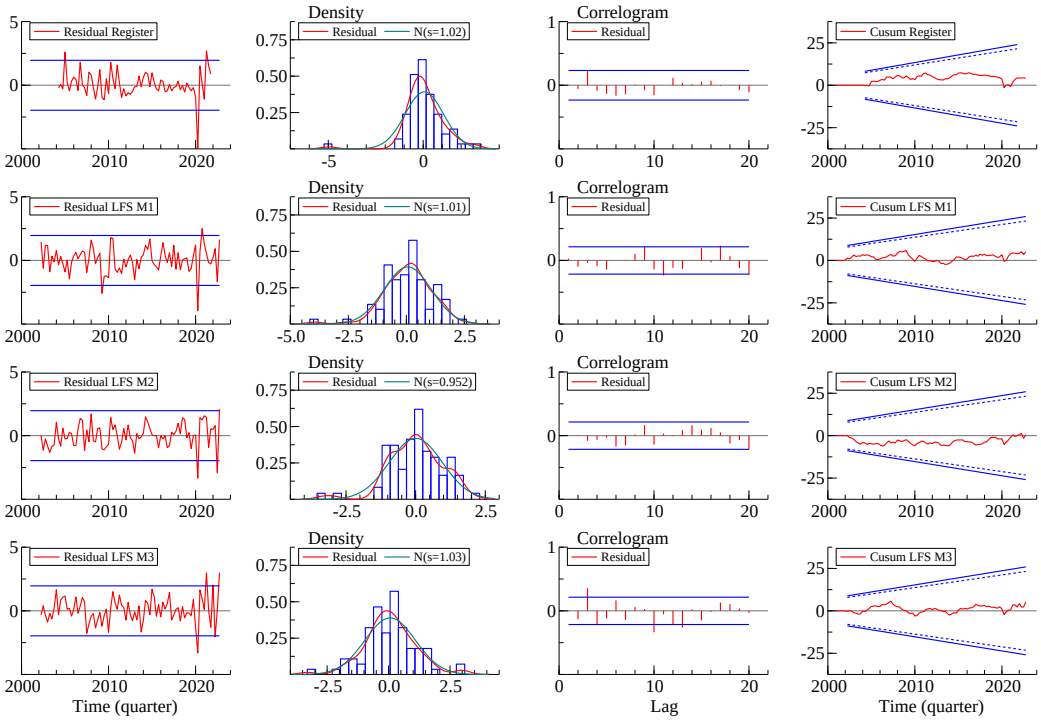


Figure SC7: Innovations diagnostics of Model 4, obtained with Kalman smoother.

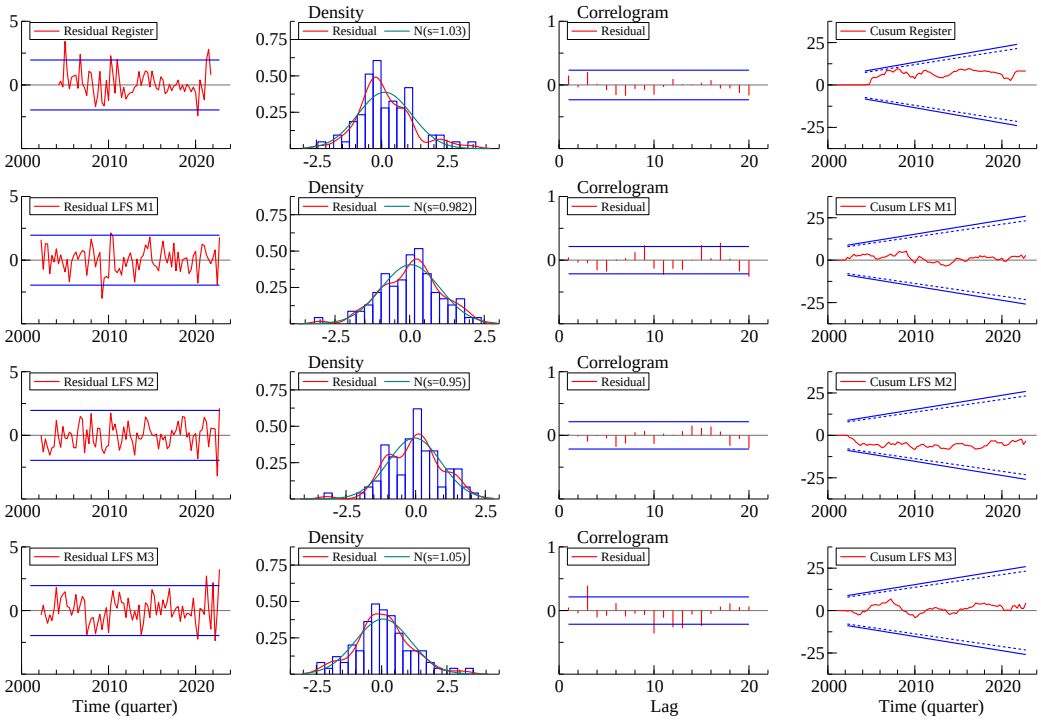


Figure SC8: Innovations diagnostics of Model 4 including time-varying variances for the trend disturbance terms at the start of the COVID-19 outbreak.

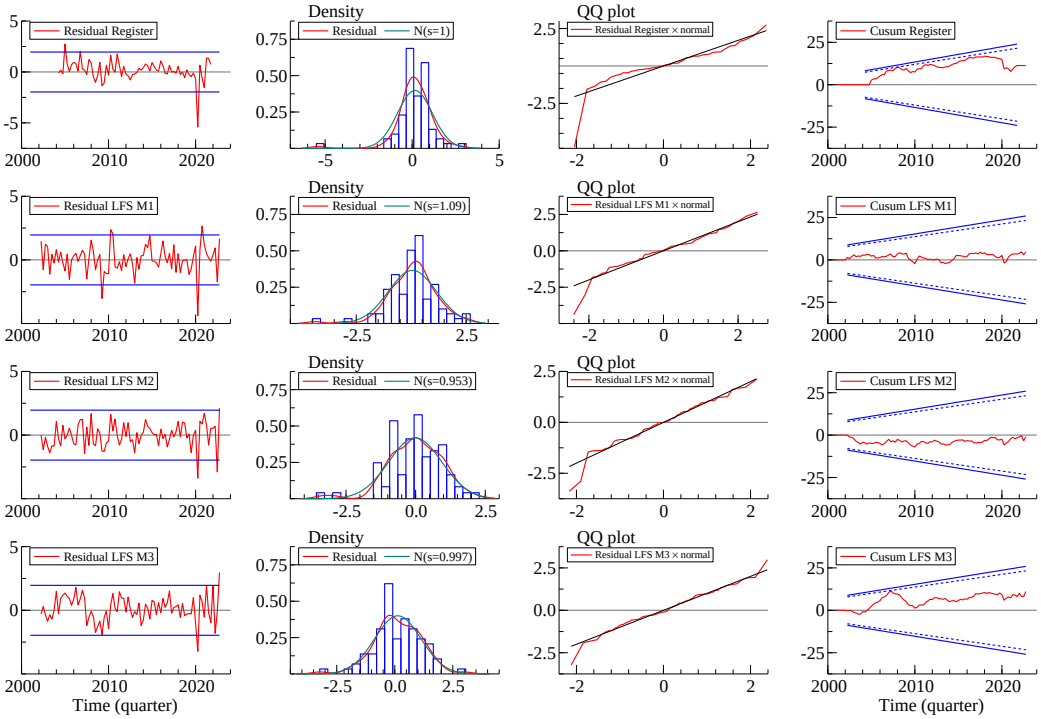


Figure SC9: Additional residual diagnostics of Model 1 with constant trend disturbance variance including QQ plot.

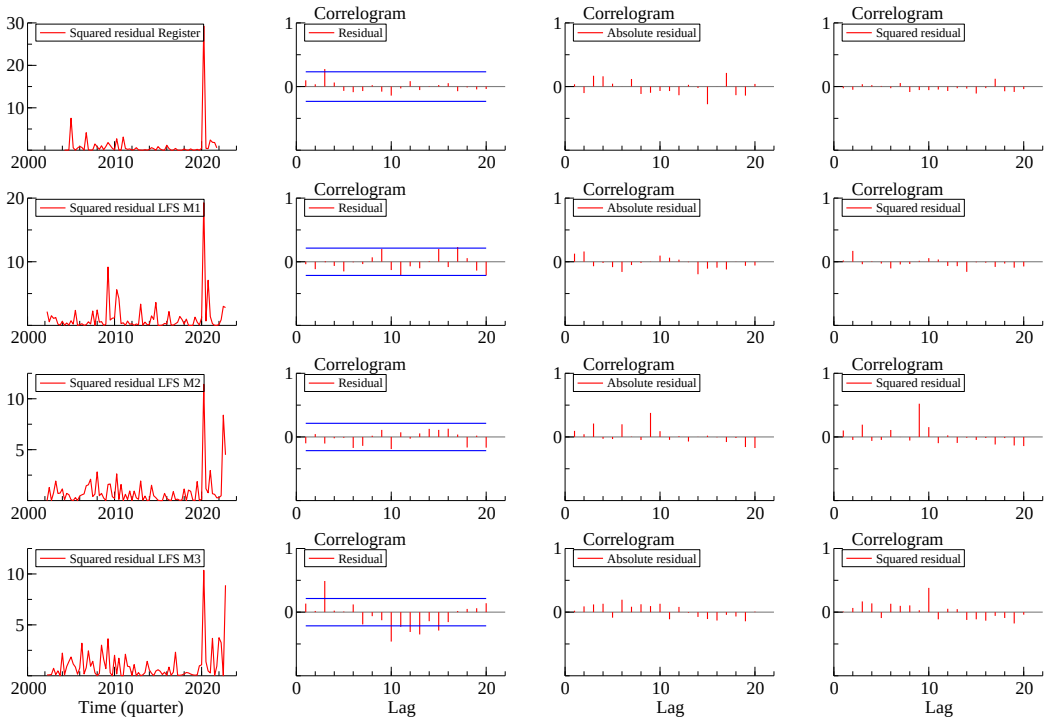


Figure SC10: Additional residual diagnostics of Model 1 with constant trend disturbance variance including autocorrelation of absolute and squared residuals.

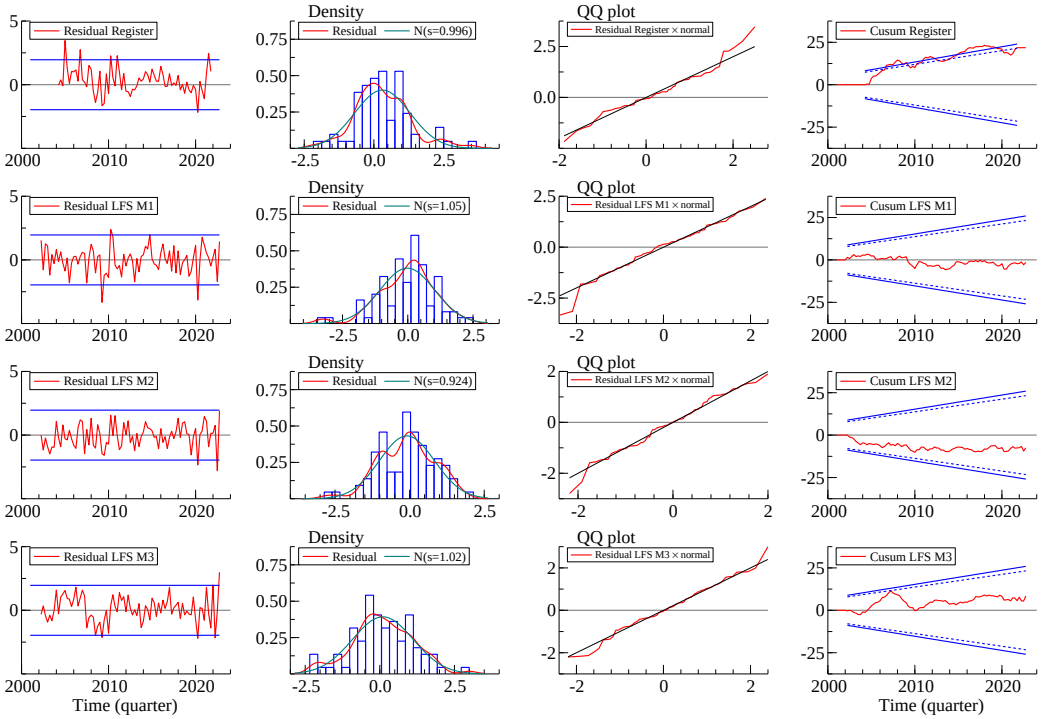


Figure SC11: Additional residual diagnostics of Model 1 with time-varying trend disturbance variance including QQ plot.

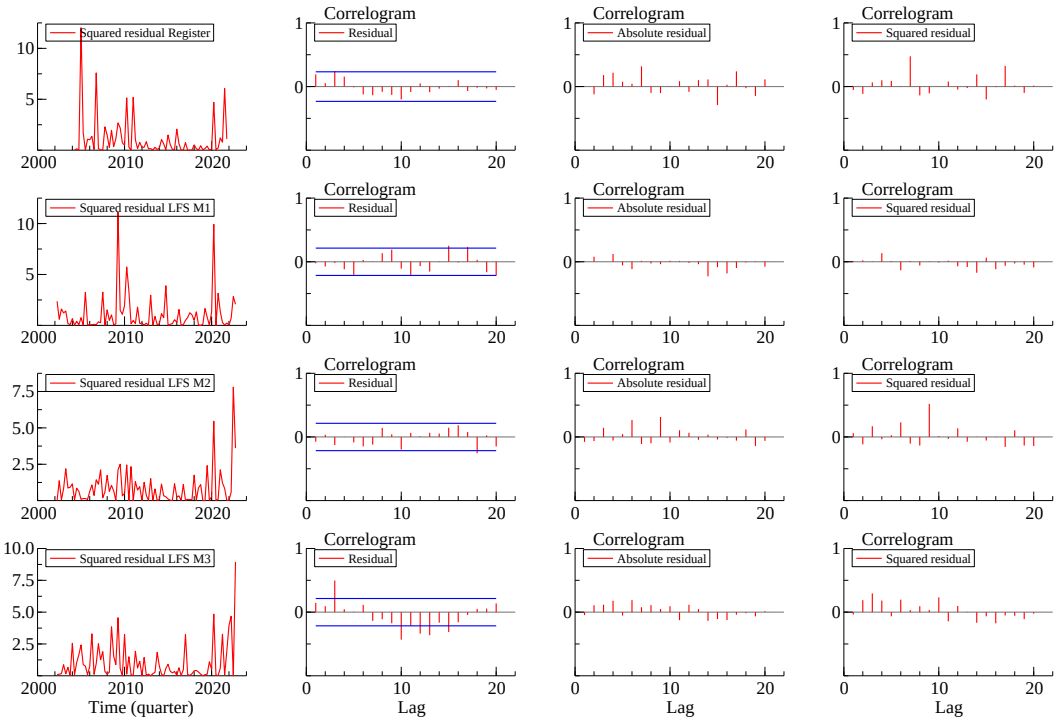


Figure SC12: Additional residual diagnostics of Model 1 with time-varying trend disturbance variance including autocorrelation of absolute and squared residuals.

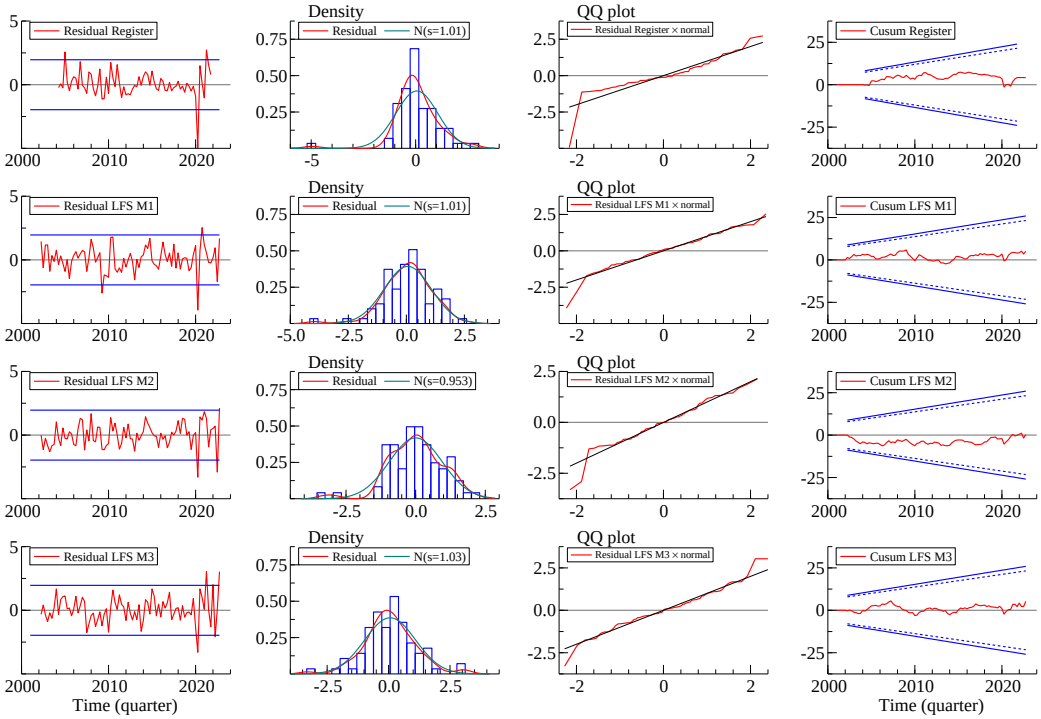


Figure SC13: Additional residual diagnostics of Model 3 with constant trend disturbance variance including QQ plot.

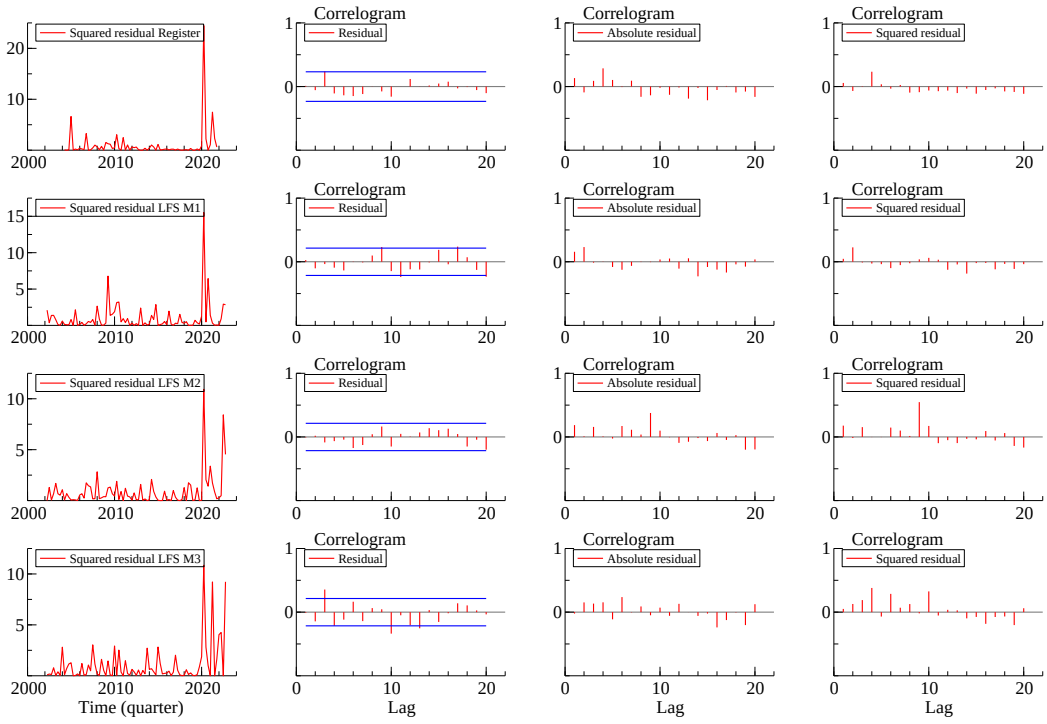


Figure SC14: Additional residual diagnostics of Model 3 with constant trend disturbance variance including autocorrelation of absolute and squared residuals.

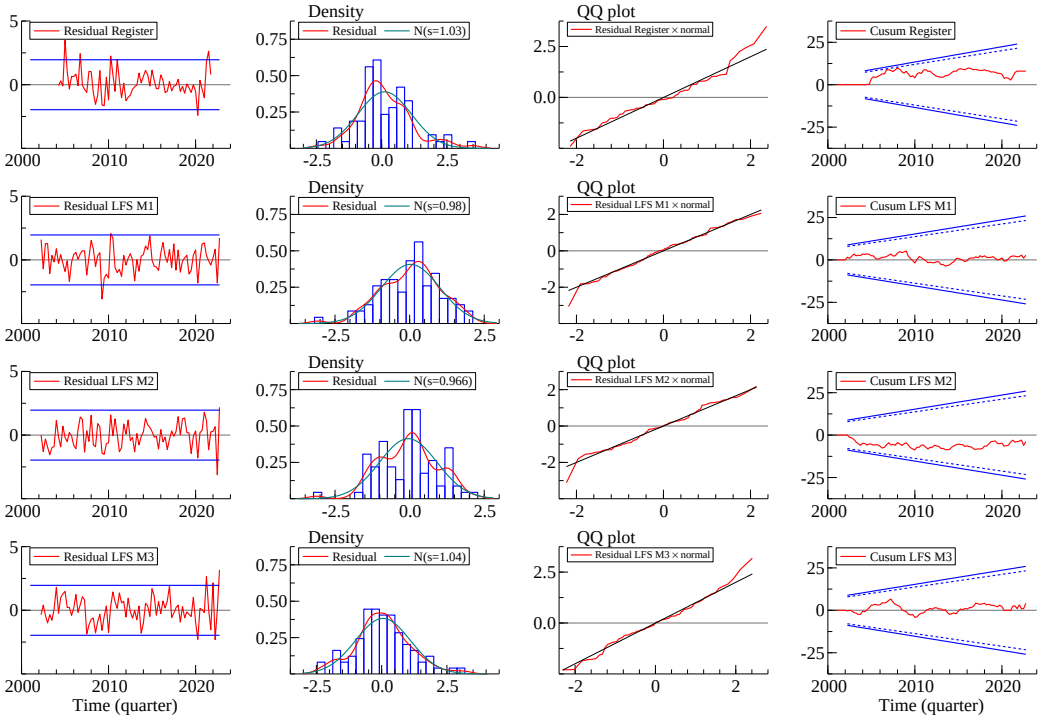


Figure SC15: Additional residual diagnostics of Model 3 with time-varying trend disturbance variance including QQ plot.

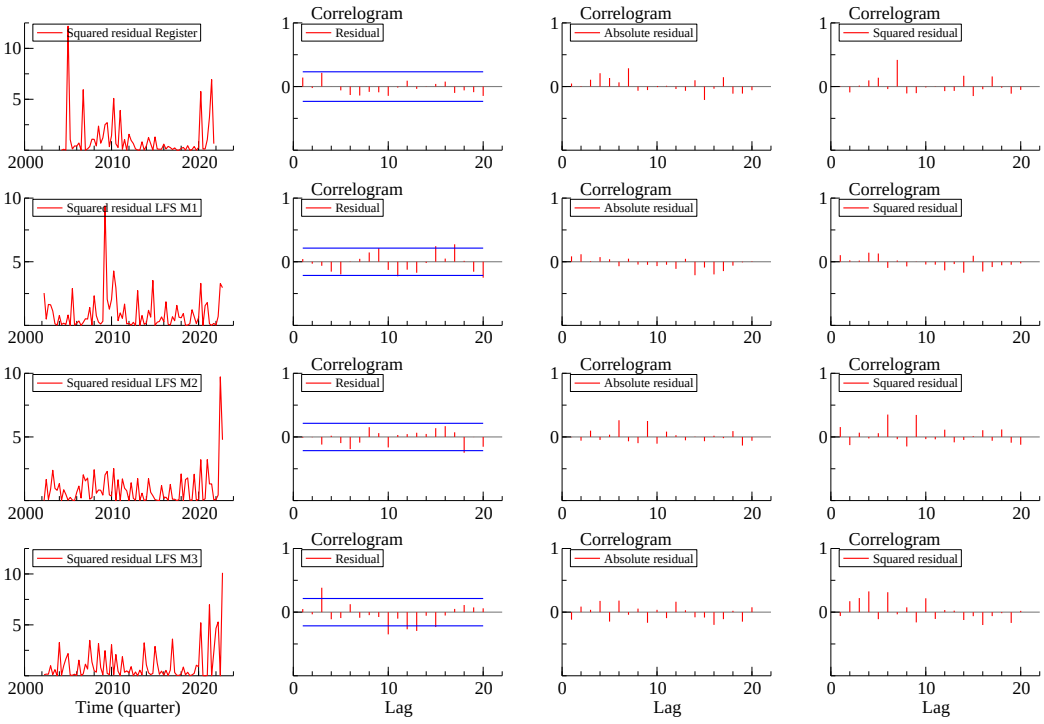


Figure SC16: Additional residual diagnostics of Model 3 with time-varying trend disturbance variance including autocorrelation of absolute and squared residuals.

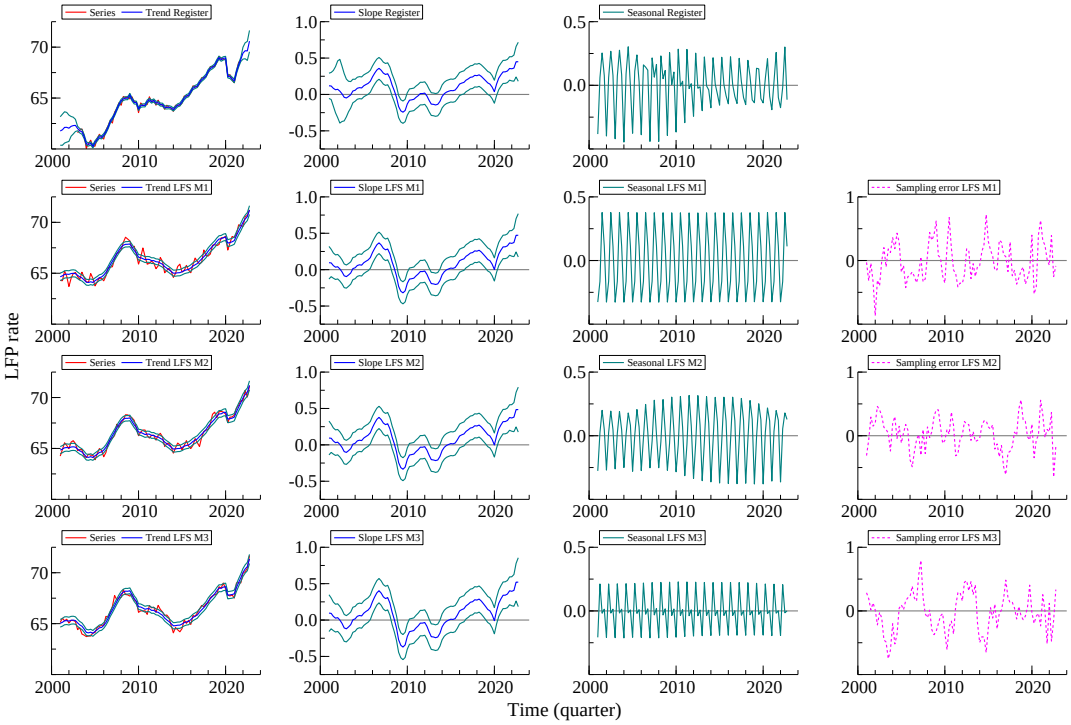


Figure SC17: State vector estimates in Model 1, obtained with Kalman smoother.

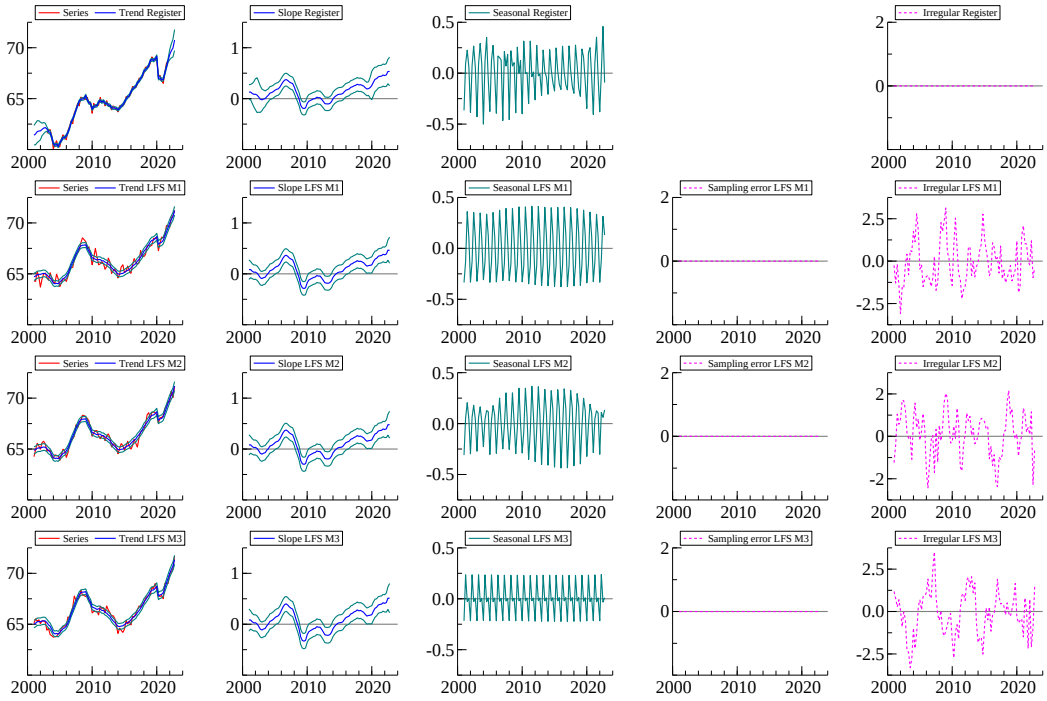


Figure SC18: State vector estimates in Model 1 including time-varying variances for the trend disturbance terms at the start of the COVID-19 outbreak.

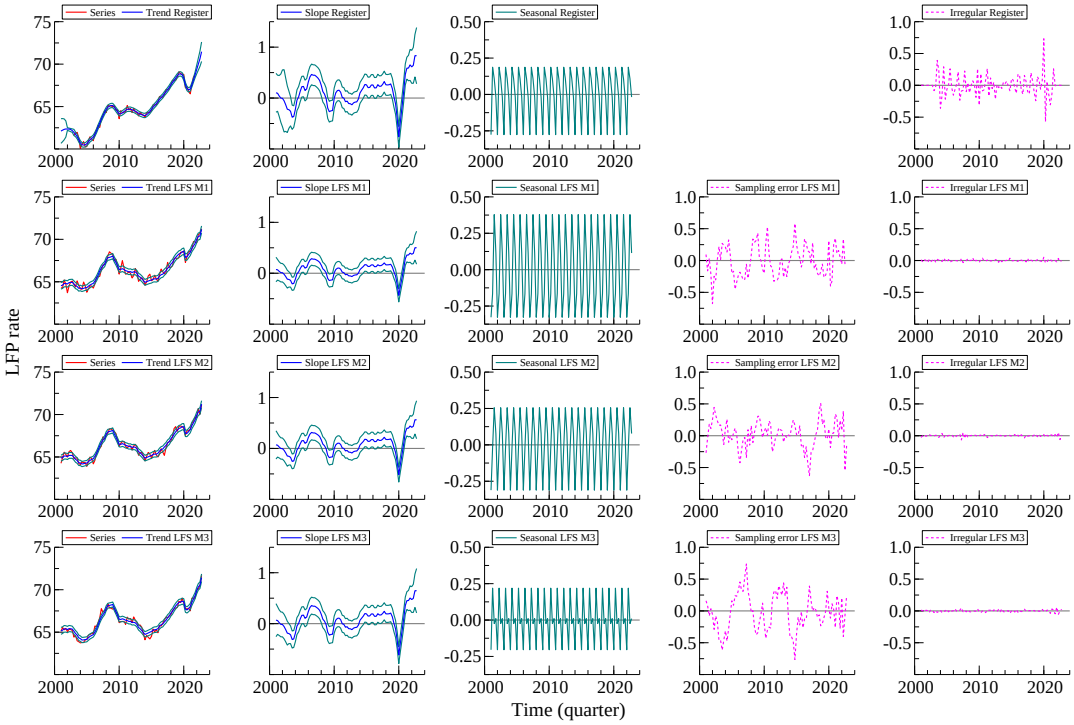


Figure SC19: State vector estimates in Model 2, obtained with Kalman smoother.

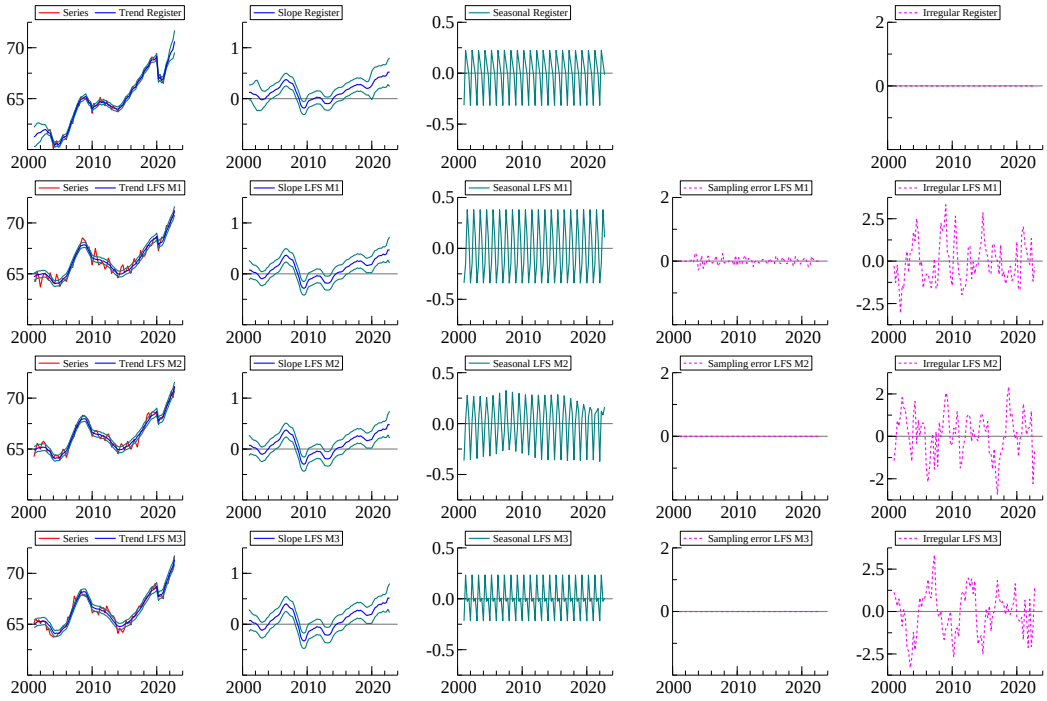


Figure SC20: State vector estimates in Model 2 including time-varying variances for the trend disturbance terms at the start of the COVID-19 outbreak.

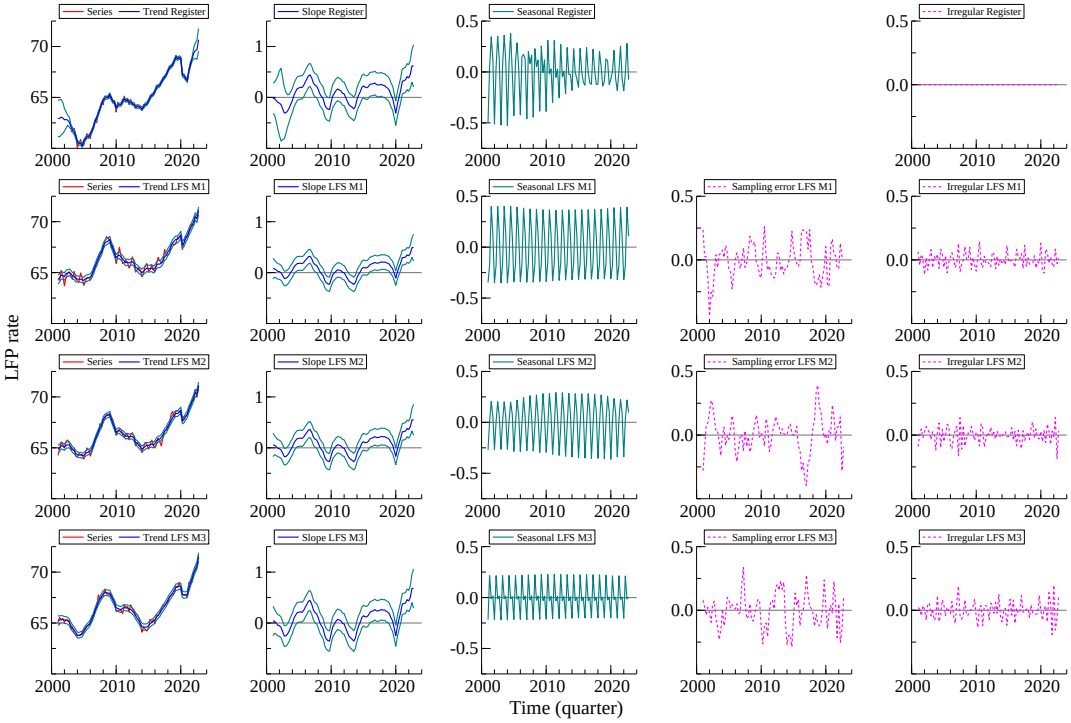


Figure SC21: State vector estimates in model 3 with constant variances for the trend disturbance terms, obtained with Kalman smoother.

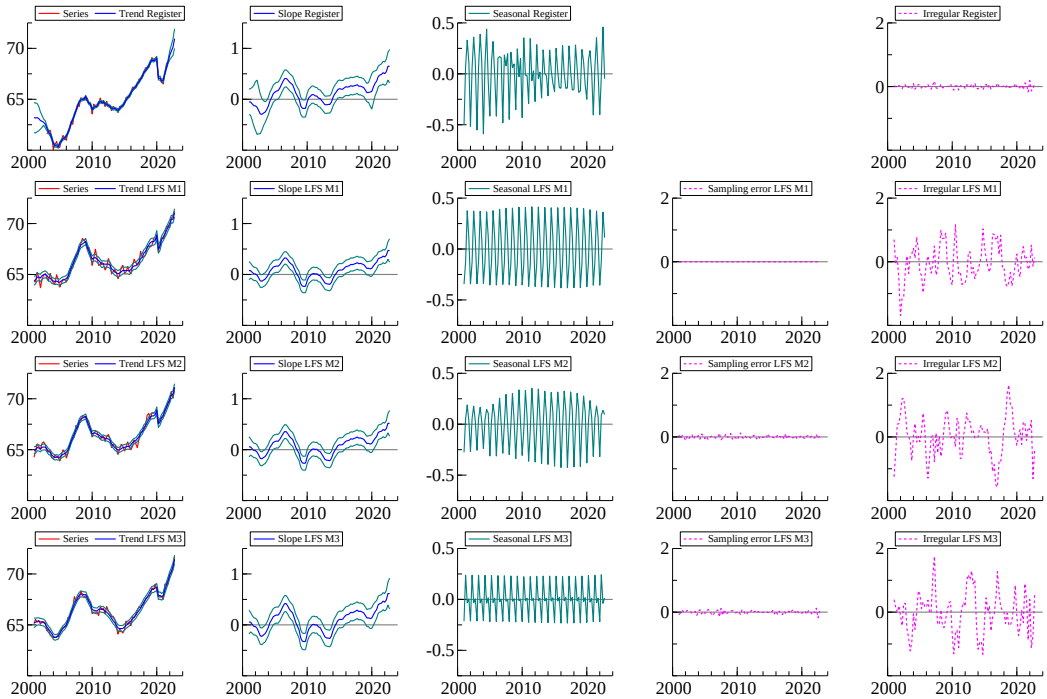


Figure SC22: State vector estimates in model 3 including time-varying variances for the trend disturbance terms at the start of the COVID-19 outbreak.

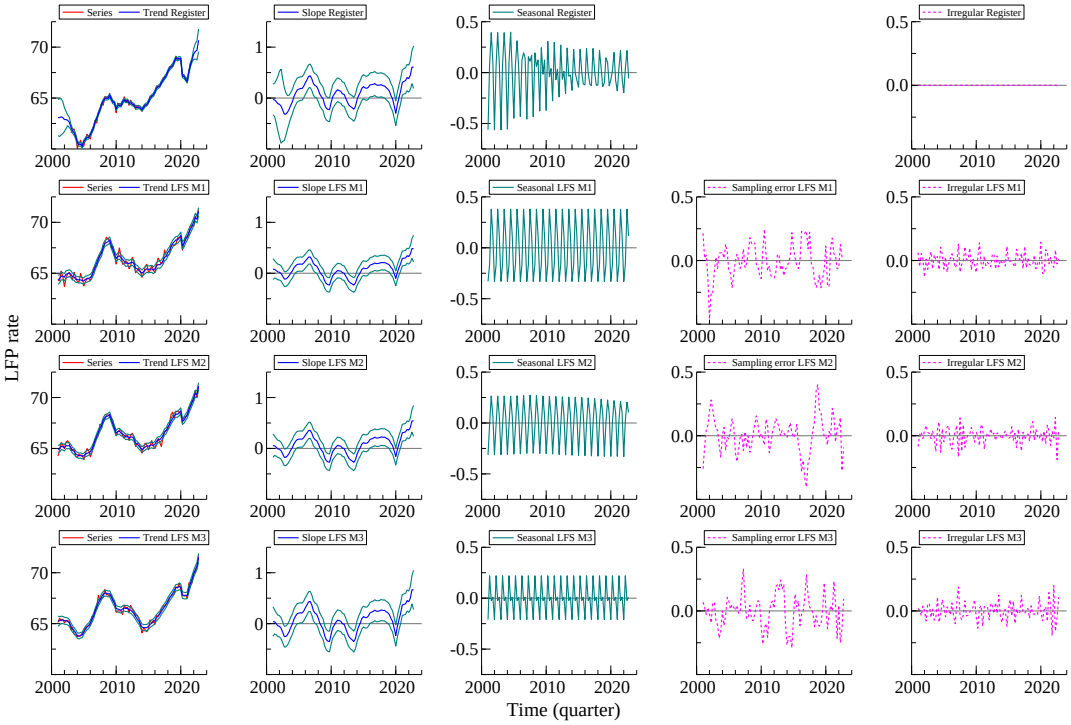


Figure SC23: State vector estimates in Model 4, obtained with Kalman smoother.

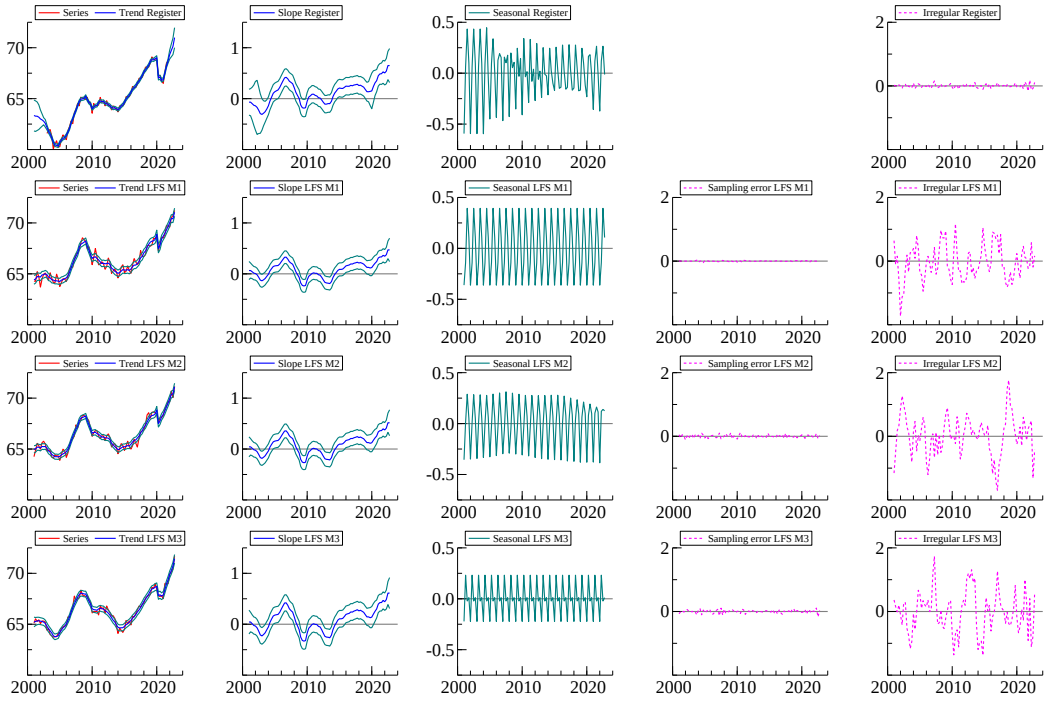


Figure SC24: State vector estimates in Model 4 including time-varying variances for the trend disturbance terms at the start of the COVID-19 outbreak.

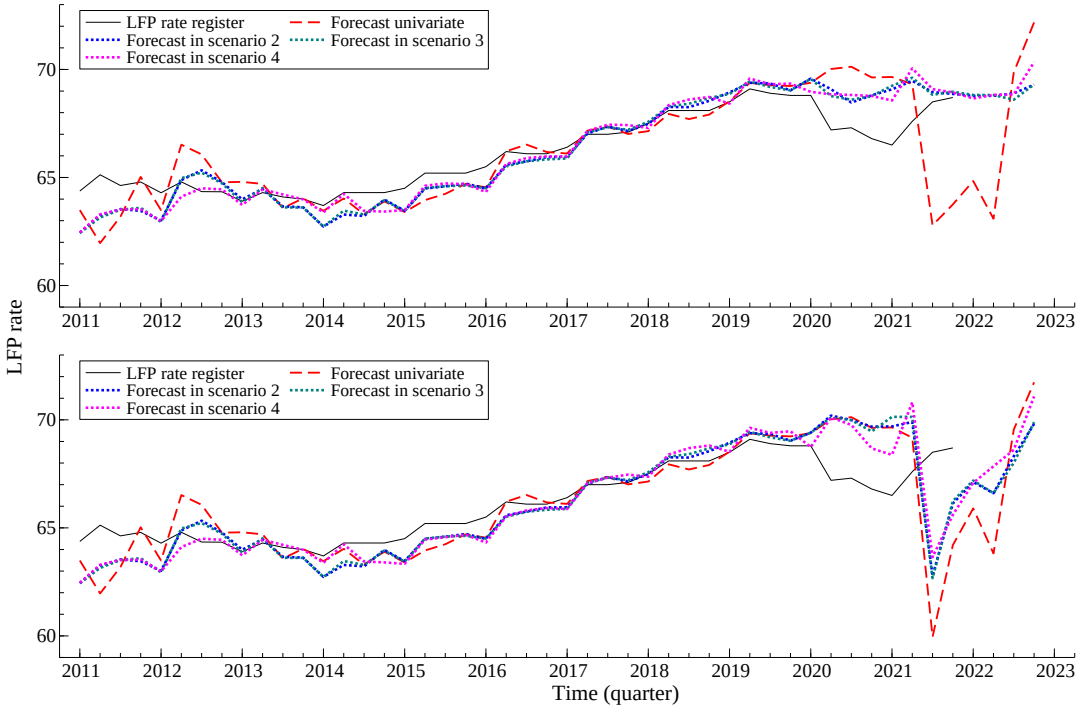


Figure SC25: 5-step ahead forecasts of the register LPF rate series of Model 1, in the different forecast scenarios, constant (top) and time-varying (bottom) variances for trend disturbance terms.

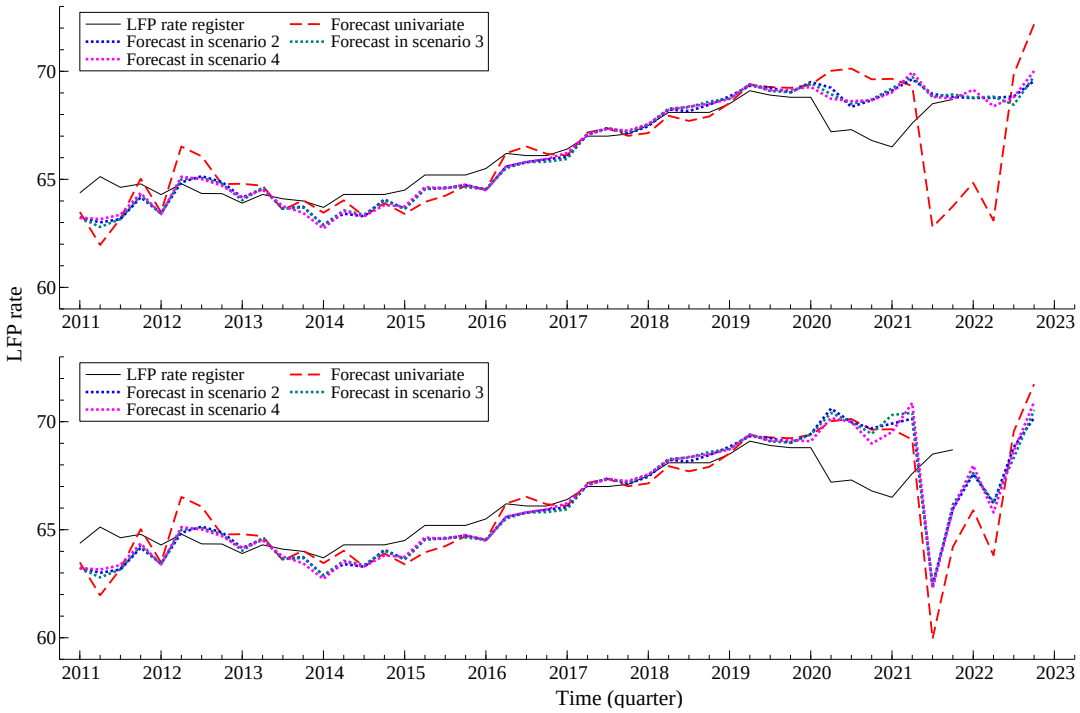


Figure SC26: 5-step ahead forecasts of the register LPF rate series of Model 2, in the different forecast scenarios, constant (top) and time-varying (bottom) variances for trend disturbance terms.

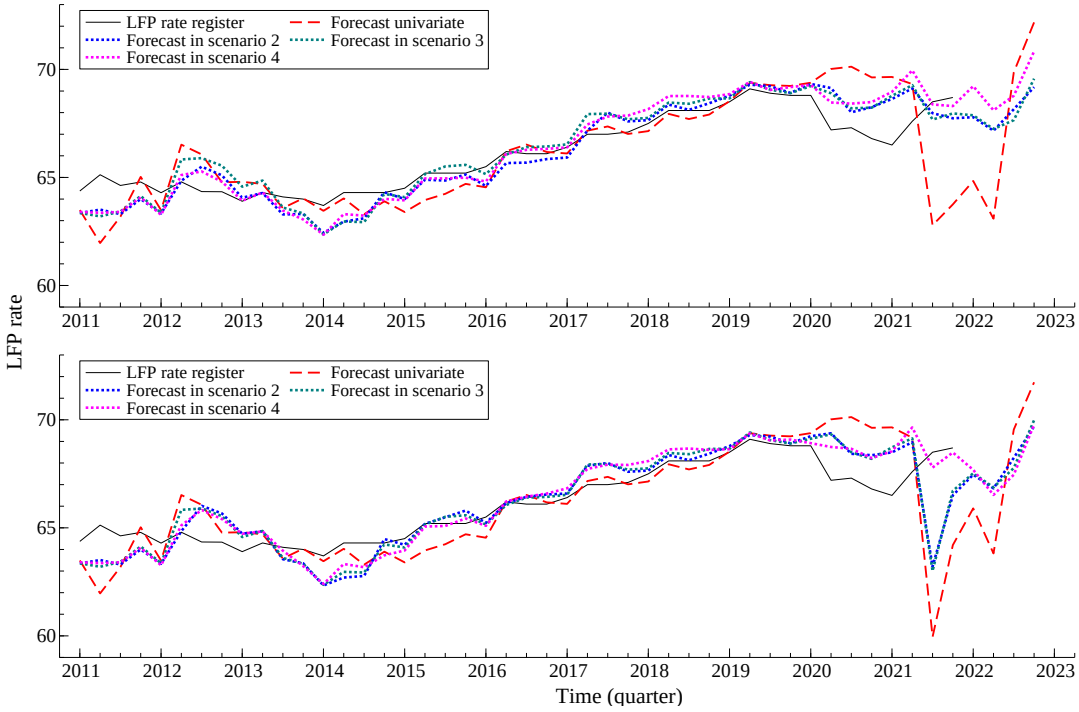


Figure SC27: 5-step ahead forecasts of the register LPF rate series of Model 4, in the different forecast scenarios, constant (top) and time-varying (bottom) variances for trend disturbance terms.

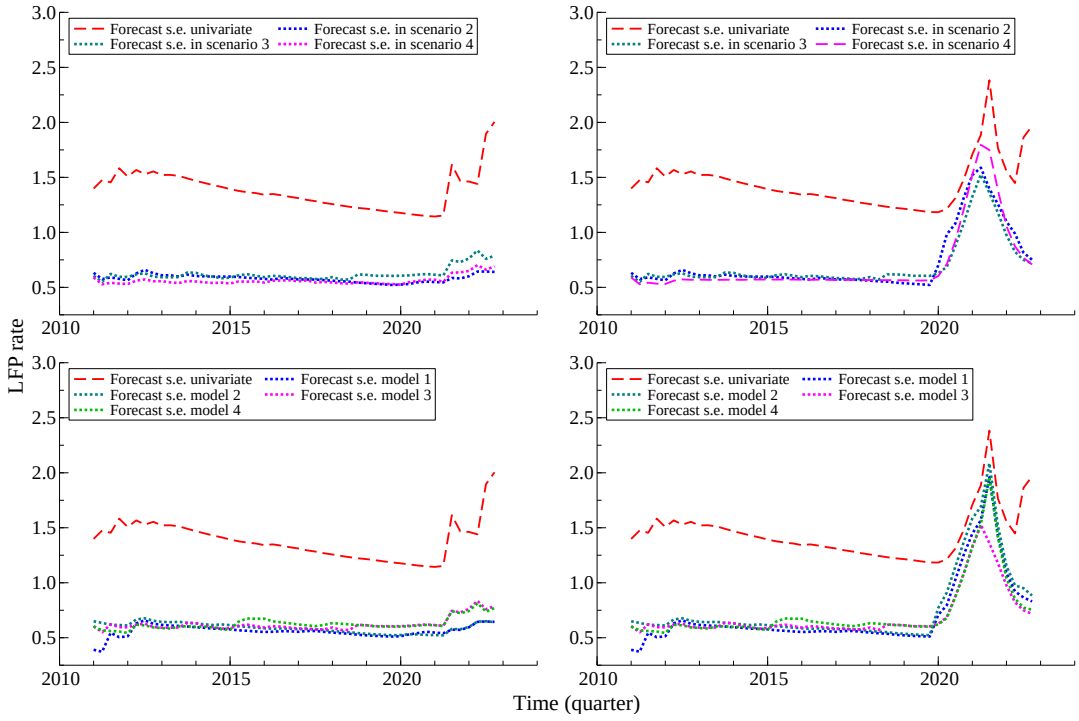


Figure SC28: Forecast standard errors comparison from model 3 in the different scenarios and of the different models in scenario 3, with constant (left) and time-varying (right) variances for trend disturbance terms.

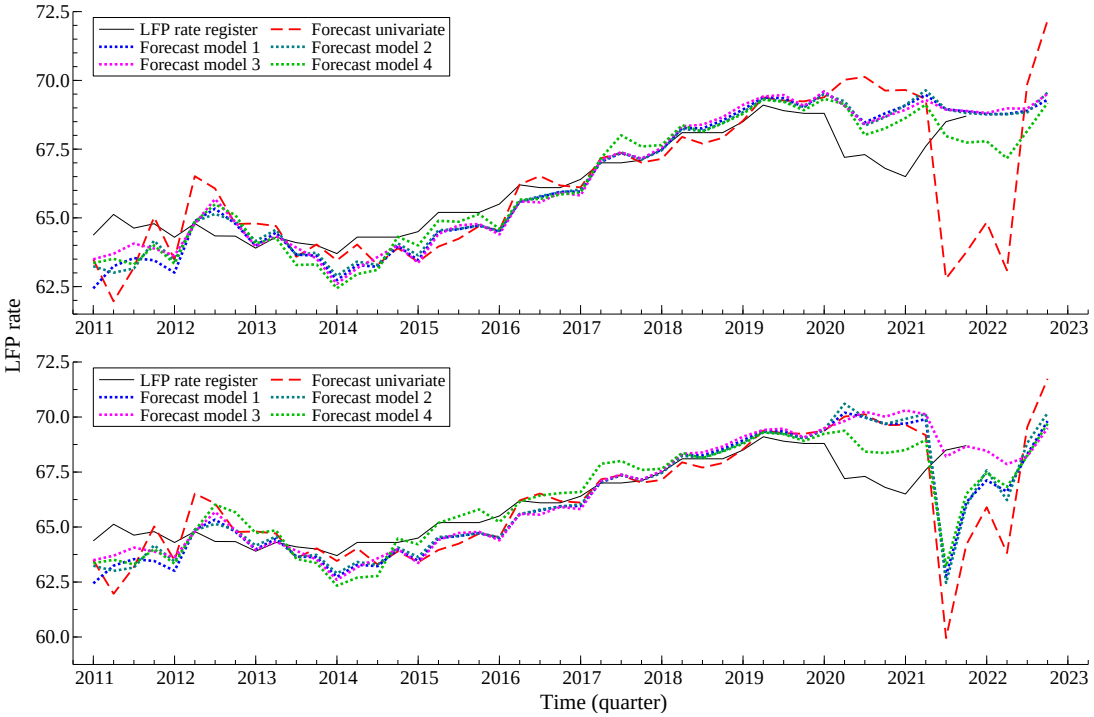


Figure SC29: 5-step ahead forecasts of the register LPF rate series of the different models, in forecasting scenario 2, constant (top) and time-varying (bottom) variances for trend disturbances.

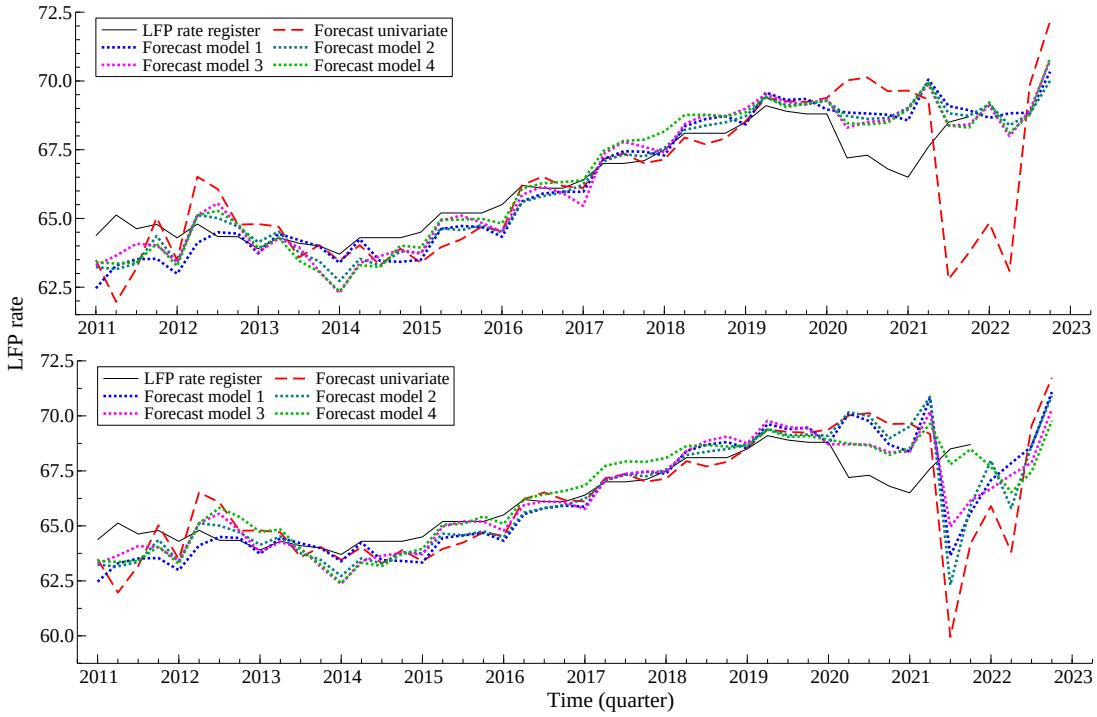


Figure SC30: 5-step ahead forecasts of the register LPF rate series of the different models, in forecasting scenario 4, constant (top) and time-varying (bottom) variances for trend disturbances.